Submitted to
Annual Review of
Nuclear Science

LBL-662
Preprint

NUCLEAR LEVEL DENSITIES

J.R. Huizenga and L.G. Moretto

March 1972

AEC Contract No. W-7405-eng-48

LBL-662

DISCLAIMER

NUCLEAR LEVEL DENSITIES

J. R. Huizenga*

Nuclear Structure Research Laboratory
University of Rochester
Rochester, New York 14627

and

L. G. Moretto*

Lawrence Berkeley Laboratory
University of California
Berkeley, California 94720

March 1972

INTRODUCTION

The levels of a nucleus can be divided into two energy regions, namely the "low energy" and "high energy" excitations. This division arises naturally from the different approach employed for their analysis: the spectroscopical approach for the low energy levels and the statistical approach for the high energy levels. The low-lying nuclear excited levels are small in number, well separated, and their structure is rather simple. For these levels the spectroscopical approach is the most suitable and leads to information concerning configurations, residual interactions and mixing.

With increasing excitation energy, the spacing between the levels is progressively reduced and the nature of the excitations becomes very complicated. The existence of such complex levels is beautifully illustrated by the neutron capture resonances. Their average spacing is about 10^6 times smaller than the

*Research supported in part by the U.S. Atomic Energy Commission.

average single particle level spacing and their widths are also 10^6 times smaller than expected for a single particle excitation (1). This and other evidence indicate that a large number of degrees of freedom is involved, with considerable configuration mixing. These experimental observations support the concept of the compound nucleus introduced by N. Bohr (2,3). In this description the reacting system (nucleus + neutron) relaxes via two-body interactions to a highly complex configuration called the compound nucleus, which has no memory of the original reaction, except for the constants of motion.

Because of these considerations and experimental observations, it is natural that, for nuclei with increasing excitation energy, the spectroscopic approach should be abandoned in favor of a statistical approach which allows a more comprehensive description of the average behavior of the compound nucleus and of its decay. In particular the decay process of the compound nucleus becomes controlled by the phase space of the "products" and the matrix elements between the different states become averaged by the sheer number of levels and by their very high density (4,5).

The most relevant quantity describing the statistical nuclear properties is then the level density of the system, expressed as a function of the various

constants of motion like excitation energy, number of particles, angular momentum, parity, isospin, etc. A special kind of level density, important in the description of the nuclear relaxation towards equilibrium is the level density for a fixed number of particles and holes.

In the present article a distinction is made between level density and state density. The former refers to nuclear levels irrespective of their angular momentum degeneracy and is indicated by $\rho(E)$; the latter accounts for the $2I + 1$ degeneracy of the levels and is indicated by $\omega(E)$.

The present paper will be divided into two main sections. The first part will outline the main methods and models which have been used for the calculation of the theoretical level densities. The second will deal with the sources of experimental information for the level density.

THEORETICAL OUTLINE OF THE METHODS AND MODELS EMPLOYED IN THE EVALUATION OF LEVEL DENSITIES

To some extent, the models used in the level density calculations have followed the evolution of the knowledge of the nuclear properties. A certain lag, which is still noticeable at present, can in part be attributed to the

complexity of the statistical calculations and to one's reluctance to abandon analytical expressions in favor of more powerful numerical methods.

Initially, the nucleus was represented as a gas of non-interacting fermions confined to the nuclear volume (Fermi gas) (7-13). More specifically, the zeroth order expansion of this model was used, which corresponds to the equidistant model (equally spaced energy levels). The equidistant model has been largely employed in data analysis and is very popular even at present although it contains little physical information.

Margenau (14) and Bloch (15) have presented a general procedure to include the shell model into level density calculations. However, a large amount of effort has been devoted to the development of semiempirical approaches to the problem, either by modifying the parameters of the equidistant model formula (16,17), or by introducing a shell correction in terms of an energy shift in the ground state (18,19). A more fundamental attempt to understand the effect of the shell model degeneracies has been made with the Rosenzweig degenerate model (20,21). In the same spirit more sophisticated models based on schematic single particle level sequences have been studied (22-29) also.

The application of the pairing Hamiltonian to excited nuclei has provided a further improvement in the understanding of the low energy behavior of the level density (10,30-34). The most recent studies in the field have profited from the use of numerical methods for the evaluation of level densities directly from the shell model single particle level schemes (14,35-42). Furthermore numerical calculations have been performed to evaluate level densities on the basis of the shell model single particle scheme and the pairing Hamiltonian as well (43-47). Ab initio calculations including in a consistent way the nuclear deformation as well as the shell model and the pairing Hamiltonian are also possible (48,49).

To a large extent, the nuclear models employed in the level density calculation have been determined by one's ability to find suitable methods of calculation. Therefore the most common methods of calculation will be illustrated before describing in some detail the models themselves.

Methods of Calculation

The Combinatorial Method.--

The combinatorial approach is suggested by the definition of the level density. For a system of non interacting fermions, this method amounts to

finding the number of ways in which the nucleons can be distributed among the available single particle levels for a fixed energy of the system. A few authors have used this method in limited calculations (35-38). A very extended calculation has been performed by Hillman and Grover (44). In their calculation all the possible configurations are obtained by means of a simple method of enumeration and classification. The configurations are generated by cycling the occupation number of each of the single particle levels over all its allowable values. The levels are then sorted out in terms of particle number, energy and angular momentum (and possibly other quantum numbers). This method has been generalized to evaluate the level density with the inclusion of the pairing interaction.

The advantages of such a procedure are related to the fact that an "exact" counting is performed. The disadvantages arise from the extremely high value that the level densities can reach. Typically, in a heavy nucleus far from a closed shell, the level density may be of the order of 10^6 levels/MeV at the neutron binding energy. Therefore such calculations can be performed only with large computers and are limited to small excitation energies especially for heavy nuclei.

The Partition Function Method.--

This very powerful method (50) has become a classical tool in statistical mechanics due to its generality and flexibility. Let the nucleus be defined by its neutron and proton numbers N and Z and by its energy E. The statistical properties of the system are contained in the grand partition function:

$$e^{\Omega} = \sum_{N',Z',E'} \exp(\alpha_N N' + \alpha_Z Z' - \beta E') \quad , \qquad 1.$$

where α_N, α_Z, and β are Lagrange multipliers associated with the particle numbers and energy. Of particular significance is the quantity $t = \frac{1}{\beta}$ which is commonly known as the statistical temperature.

The summation is over all nuclei with N' neutrons and Z' protons, and over all the energy eigenvalues E' of each nucleus. The sum over the energy eigenstates can be substituted by an integral:

$$e^{\Omega} = \sum_{N',Z'} \int dE' \, \omega(E',N',Z') \exp(\alpha_N N' + \alpha_Z Z' - \beta E') \quad . \qquad 2.$$

The quantity $\omega(E',N',Z')$ represents the density of energy eigenvalues for the nucleus (N', Z') at the energy E', or, in other words, the state density. The above equation also shows that the grand partition function can be considered a Laplace transform of the state density. A very elegant method for the inversion

of Equation (2) in the case of a system of non interacting Fermions has been described by Williams (39). This method uses recursion relations for the calculation of the coefficients of a finite order partition function and yields the exact state density. The method can be generalized to account for quantum numbers which can be expressed in terms of sums over single particle levels. A more general method yielding the state density makes use of the inverse Laplace transform of Equation (2):

$$\omega(E,N,Z) = \frac{1}{(2\pi i)^3} \oint d\alpha_N \oint d\alpha_Z \oint d\beta \; e^S \quad , \qquad 3.$$

where $S = \Omega - \alpha_N N - \alpha_Z Z + \beta E$. The above contour integrals are also known as the Darwin-Fowler integrals. So far the only approximation introduced into the calculation is the continuous approximation whereby the state density is considered a continuous function. However, the generality of the method arises from a remarkable approximation which allows one to evaluate the integrals in Equation (3).

It can be shown that the integrand has a saddle point whose location is defined by the equations:

$$\frac{\partial S}{\partial \alpha_N} = 0 \; ; \qquad \frac{\partial S}{\partial \alpha_Z} = 0 \; ; \qquad \frac{\partial S}{\partial \beta} = 0$$

or

$$\frac{\partial \Omega}{\partial \alpha_N} = N \; ; \qquad \frac{\partial \Omega}{\partial \alpha_Z} = Z \; ; \qquad \frac{\partial \Omega}{\partial \beta} = -E \quad . \qquad 4.$$

The paths of integration can be chosen to pass through this point. By expanding the exponent S in a Taylor series about the saddle point and retaining only the quadratic terms, the integrals in Equation (3) yield the following result:

$$\omega(E,N,Z) = \frac{\exp S}{(2\pi)^{3/2} \, D^{1/2}} \quad , \qquad 5.$$

where D is a 3×3 determinant of the second derivatives of Ω with respect to the Lagrange multipliers α_N, α_Z and β. All of the quantities contained in Equation (5) must be evaluated at the saddle point.

Such an approximation corresponds to the Stirling approximation for the evaluation of factorials and its accuracy depends upon the magnitude of the state density itself. The agreement of results based upon the saddle point approximation with the exact results is good even at low excitation energies (42). The elegance of the method is also quite apparent in the way

in which the boundary conditions of the problem are introduced. They appear in a very simple way in Equations (4) where the saddle point location is defined.

This procedure can be generalized for an arbitrary number of constants of motion κ_i. If n constants are introduced, the state density retains the form of Equation (5) where $S = \Omega + \beta E - \sum_{i=1}^{n-1} \alpha_1 \kappa_1$ and the exponent of 2π is n/2. The quantity D is now an nxn determinant of the second derivatives of Ω with respect to α_i and β. All the quantities α_i and β are evaluated at the saddle point.

Nuclear Models

System of Non-Interacting Fermions.--

For such a system, the grand partition function can be easily evaluated. Let the energy levels be represented by a_K for neutrons and b_K for protons; let also the magnetic quantum numbers for neutrons and protons be m_{1K} and m_{2K}, respectively. The constants of motion are the neutron and proton numbers N and Z, the energy E and the projection of the angular momentum on a space-fixed axis, M. The logarithm of the grand partition function is:

$$\Omega = \sum \ln[1 + \exp(\alpha_N + \mu\, m_{1K} - \beta\, a_K)] + \sum \ln[1 + \exp(\alpha_2 + \mu\, m_{2K} - \beta\, b_K)] \quad . \quad 6.$$

The saddle point is defined by the following equations:

$$N = \sum \frac{1}{1 + \exp - (\alpha_N + \mu\, m_{1K} - \beta\, a_K)} \; ; \; Z = \sum \frac{1}{1 + \exp - (\alpha_Z + \mu\, m_{2K} - \beta b_K)}$$

$$M = \sum \frac{m_{1K}}{1 + \exp - (\alpha_N + \mu\, m_{1K} - \beta\, a_K)} + \sum \frac{m_{2K}}{1 + \exp - (\alpha_Z + \mu\, m_{2K} - \beta\, b_K)}$$

$$E = \sum \frac{a_K}{1 + \exp - (\alpha_N + \mu\, m_{1K} - \beta\, a_K)} + \sum \frac{b_K}{1 + \exp - (\alpha_Z + \mu\, m_{2K} - \beta\, b_K)} \quad 7.$$

The entropy is given by:

$$S = \sum \ln[1 + \exp + (\alpha_N + \mu\, m_{1K} - \beta\, a_K)] + \sum \ln[1 + \exp + (\alpha_Z + \mu\, m_{2K} - \beta\, b_K)]$$

$$+ \sum \frac{\beta\, a_K - \alpha_N - \mu\, m_{1K}}{1 + \exp - (\alpha_N + \mu\, m_{1K} - \beta\, a_K)} + \sum \frac{\beta\, b_K - \alpha_Z - \mu\, m_{2K}}{1 + \exp - (\alpha_Z + \mu\, m_{2K} - \beta\, b_K)} \quad . \quad 8.$$

The second derivatives which appear in the 4×4 determinant in the denominator of the state density formula are:

$$\frac{\partial^2 \Omega}{\partial \alpha_N^{\,2}} = \frac{1}{4} \sum \operatorname{sech}^2 \frac{1}{2} (\beta\, a_K - \alpha_N - \mu\, m_{1K})$$

$$\frac{\partial^2 \Omega}{\partial \alpha_Z^{\,2}} = \frac{1}{4} \sum \operatorname{sech}^2 \frac{1}{2} (\beta\, b_K - \alpha_Z - \mu\, m_{2K})$$

$$\frac{\partial^2\Omega}{\partial\beta^2} = \frac{1}{4}\sum a_\kappa^2 \operatorname{sech}^2 \frac{1}{2}(\beta a_\kappa - \alpha_N - \mu m_{1\kappa}) + \frac{1}{4}\sum b_\kappa^2 \operatorname{sech}^2 \frac{1}{2}(\beta b_\kappa - \alpha_Z - \mu m_{2\kappa})$$

$$\frac{\partial^2\Omega}{\partial\mu^2} = \frac{1}{4}\sum m_{1\kappa}^2 \operatorname{sech}^2 \frac{1}{2}(\beta a_\kappa - \alpha_N - \mu m_{1\kappa}) + \frac{1}{4}\sum m_{2\kappa}^2 \operatorname{sech}^2 \frac{1}{2}(\beta b_\kappa - \alpha_Z - \mu m_{2\kappa})$$

$$\frac{\partial^2\Omega}{\partial\alpha_N\partial\alpha_Z} = 0 \quad .$$

$$\frac{\partial^2\Omega}{\partial\alpha_N\partial\mu} = \frac{1}{4}\sum m_{1\kappa} \operatorname{sech}^2 \frac{1}{2}(\beta a_\kappa - \alpha_N - \mu m_{1\kappa})$$

$$\frac{\partial^2\Omega}{\partial\alpha_Z\partial\mu} = \frac{1}{4}\sum m_{2\kappa} \operatorname{sech}^2 \frac{1}{2}(\beta b_\kappa - \alpha_Z - \mu m_{2\kappa})$$

$$\frac{\partial^2\Omega}{\partial\alpha_N\partial\beta} = -\frac{1}{4}\sum a_\kappa \operatorname{sech}^2 \frac{1}{2}(\beta a_\kappa - \alpha_N - \mu m_{1\kappa})$$

$$\frac{\partial^2\Omega}{\partial\alpha_Z\partial\beta} = -\frac{1}{4}\sum b_\kappa \operatorname{sech}^2 \frac{1}{2}(\beta b_\kappa - \alpha_Z - \mu m_{2\kappa})$$

$$\frac{\partial^2\Omega}{\partial\mu\partial\beta} = -\frac{1}{4}\sum m_{1\kappa} a_\kappa \operatorname{sech}^2 \frac{1}{2}(\beta a_\kappa - \alpha_N - \mu m_{1\kappa})$$

$$- \frac{1}{4}\sum m_{2\kappa} b_\kappa \operatorname{sech}^2 \frac{1}{2}(\beta b_\kappa - \alpha_Z - \mu m_{2\kappa}) \quad .$$

Because of the importance and simplicity of the present case, the formalism has been reported in its entirety. The above formalism allows one to calculate

the state density for a nucleus specified by N neutrons, Z protons, total energy E and angular momentum projection M. An approximate expression for $\omega(E,N,Z,M)$ is the following:

$$\omega(E,N,Z,M) = \omega(E,N,Z) \frac{\exp(-M^2/2\sigma^2)}{\sqrt{2\pi\sigma^2}} \quad , \qquad 9.$$

where $\omega(E,N,Z)$ is obtained from the previous formalism by eliminating the Lagrange multiplier μ. The quantity σ^2, called the spin cut-off parameter, determines the width of the M distribution and is given by the expression:

$$\sigma^2 = \frac{1}{4} \sum m_{1K} \operatorname{sech}^2 \frac{1}{2} (\beta a_K - \alpha_N) + \frac{1}{4} \sum m_{2K} \operatorname{sech}^2 \frac{1}{2} (\beta b_K - \alpha_Z) \quad . \quad 10.$$

As suggested by Bethe (7), the dependence of the level density upon the total angular momentum I is given by:

$$\rho(E,N,Z,I) = \omega(E,N,Z,M = I) - \omega(E,N,Z,M = I + 1) \quad , \qquad 11.$$

or

$$\rho(E,N,Z,I) = - \left[\frac{d}{dM} \omega(E,N,Z,M)\right]_{M = I + \frac{1}{2}} \simeq \frac{2I + 1}{2(2\pi)^{1/2}\sigma^3} \omega(E,N,Z) \exp\left[- \frac{(I + 1/2)^2}{2\sigma^2}\right] . \qquad 12.$$

The evaluation of the level density within the present formalism is dependent upon the solution of the saddle point equations which yield the quantities α_N,

α_Z, μ, β. Since, in general, the saddle point equations are non-linear, they must be solved numerically. However there are some highly simplified cases where the level density can be expressed analytically.

The Equidistant Model.--

In this model (7-13) the single particle levels are equidistant and non-degenerate. The total state density for a system composed of two kinds of particles is given approximately in analytical form by:

$$\omega(E) \simeq \frac{\sqrt{\pi}}{12} \frac{\exp 2\sqrt{aE}}{E^{5/4}\, a^{1/4}} \quad , \qquad 13.$$

where $a = \frac{\pi^2}{6} g$ and g is the single particle level density. The explicit dependence of the state density upon excitation energy arises from the simple relation between excitation energy and statistical temperature:

$$E = at^2 \quad .$$

Such an expression, or equivalent ones, has been widely used because of its simplicity although the model it is based upon is quite unrealistic. It is also sometimes described as the Fermi gas level density expression. This is incorrect: in a Fermi gas, the single particle level density increases

approximately as the square root of the particle kinetic energy while in the present model it is a constant. Such an expression is only the zeroth order approximation to the level density of a Fermi gas.

Because of the simplicity of the equidistant model, we report here some of the formulae based on it which are widely used in data analysis (51,52). The level density for a single angular momentum and both parities as a function of the excitation energy E is given by:

$$\rho(E,I) = \frac{1}{24\sqrt{2}} \left(\frac{1}{a}\right)^{1/4} \frac{1}{\sigma^3} \frac{(2I+1)}{E^{5/4}} \exp\left\{2(aE)^{1/2} - (I+\tfrac{1}{2})^2/2\sigma^2\right\} \quad . \qquad 14.$$

The total level density is related to $\rho(E,I=0)$ by:

$$\rho(E) = 2\sigma^2 \rho(E,I=0) \quad . \qquad 15.$$

In these expressions the spin cut off parameter is given by the relation:

$$\sigma^2 = g \langle m^2 \rangle t = \frac{\mathcal{J}t}{\hbar^2} \quad , \qquad 16.$$

where $\langle m^2 \rangle$ is the average of the square of the single particle spin projections. The nuclear moment of inertia $\mathcal{J}$ is assumed to be that of a rigid sphere: $\mathcal{J} = \frac{2}{5} mA R^2$, where m is the nucleon mass, A is the mass number and the radius is given by the relation: $R = 1.2 A^{1/3}$ F.

In light nuclei, where the Coulomb effects are small, each single particle level has a further twofold degeneracy, since it can be occupied by a neutron or by a proton. This arises because of the nucleon isospin projections $(\pm \frac{1}{2})$.

In complete analogy with the treatment of the angular momentum, the level density for a total isospin projection T_z is:

$$\rho(E,T_z) = \rho(E) \frac{\exp[-T_z^2/2\sigma_{T_z}^2]}{\sqrt{2\pi}\,\sigma_{T_z}} \qquad 17.$$

where $\sigma_{T_z}^2 = \frac{1}{4} gt$. If the Coulomb effects can be disregarded, the level density for a given isospin value T is:

$$\rho(E,T) = \rho(E) \frac{2T+1}{2(2\pi)^{1/2}\,\sigma_{T_z}^3} \exp\left[-\frac{(T+\frac{1}{2})^2}{2\sigma_T^2}\right] \qquad 18.$$

In problems related to the pre-equilibrium behavior of a nucleus it is necessary to calculate state densities for nuclei with fixed number of excited particles p and holes h (53,56). If a constant single particle level spacing of 1/g is assumed the energy can be expressed in dimensionless form:

$$U = gE \quad .$$

Ericson has given the following expression for the state density (54):

$$\omega(E,p,h) = \frac{g(gE)^{p+h-1}}{p!\ h!\ (p+h-1)!} \quad . \qquad 19.$$

Williams has improved the Ericson formula by properly accounting for the Pauli principle in his derivation (55). His approximate result in terms of a closed form expression is:

$$\omega(E,p,h) = \frac{g(gE-A)^{p+h-1}}{p!\ h!\ (p+h-1)!} \quad , \qquad 20.$$

where $A = \frac{1}{4}(p^2 + h^2) + \frac{1}{4}(p - h) - \frac{1}{2}h$ and has the same dimensions as gE. For this special kind of state density, shell effects are also expected to play a major role.

Level Densities for More Complex Sets of Single Particle Levels.—

The simplest system of non-equidistant levels is the Fermi gas system, where the single particle level density increases with the square root of the kinetic energy of the particles. The more general set of single particle levels given by the shell model, however, has a much more complex variation in its level spacings.

In order to simulate to some extent the bunching and the degeneracies typical of the shell model, various single particle level schemes have been

considered. A completely bunched periodical system has been explored by Rosenzweig (20). His single particle spectrum is obtained by dividing the equivalent equidistant spectrum into equal groups of levels, separated by a gap. Each group of levels is constructed to merge into one single level of fixed degeneracy, and all the resulting degenerate levels are equally spaced.

The remarkable results of this investigation show that, for high excitation energies, the level density is given by an expression equivalent to that for the equidistant model, except that an effective excitation energy E^* is substituted for E. The effective excitation energy is given by:

$$E^* = E + \frac{n^2 d_n}{12} - \frac{d_n}{2}\left(K_n - \frac{n}{2}\right)^2 + \frac{p^2 d_p}{12} - \frac{d_p}{2}\left(K_p - \frac{p}{2}\right)^2 \quad , \qquad 21.$$

where n and p are the neutron and proton level degeneracies, K_n and K_p are the neutron and proton numbers in the last occupied levels, d_n and d_p are the average spacings between neutron and proton levels, respectively. In this model the level density is lowest when the single particle levels in the ground state are completely filled or empty while it is highest when the last occupied level is half-filled. These two cases do simulate a magic nucleus and a mid-shell nucleus, respectively.

The equidistant spectrum can be partially bunched so that the groups of levels do not quite merge into a single degenerate level. It has been shown by Kahn and Rosenzweig (24,25) and by Gilbert (26) that for this model and for all the models characterized by a periodic single particle scheme, the level density at high energy can be given by a relation analogous to that of the uniform model. The effect of the shell structure can be accounted for by the substitution of an effective excitation energy for the true excitation energy:

$$E^* = E - \Delta E \quad ,$$

where ΔE is an energy shift which depends upon the structure of the ground state. If the single particle spectrum is not periodic, it is important to note that it is not possible to reduce the effects of the shell structure into a constant energy shift.

Level Densities from the Shell Model.--

All the models which have been described so far, yield analytical expressions for the level density. However, because of their unrealistic Hamiltonians, they do not predict the structure observed in the level densities near closed shells. More detailed and accurate theoretical information about

the level density is possible when one uses single particle levels obtained from a shell model calculation. These more realistic single particle levels have been used by some authors to calculate the state density by either the combinatorial approach (35-38,44) or by means of the Darwin-Fowler method (14,39-43,45-49). The last method, when coupled to the saddle point approximation as described earlier, yields perhaps the simplest and most general way of evaluating level densities in terms of the shell model.

In Figure 1 level density calculations from the Nilsson model are presented for nuclei close to ^{208}Pb (40). The shell effects appear in a remarkably clear way, indicating that the most magic nucleus ^{208}Pb has the lowest level density. The level densities increase for nuclei which are farther and farther away from the double closed shell. Also noticeable in this figure are the different excitation energy dependences of the level densities of different nuclei. In Figure 2 the spin cut-off parameters are presented for the same nuclei. The shell effects manifested in the values of σ^2 have two different origins. One origin of the shell effect is related to fluctuations in the spacings of single particle levels

and the second origin of the shell effects is related to fluctuations in the spin projection of the single particle levels. Both types of fluctuations are responsible for the strong differences in the absolute values and energy dependence of the spin cut-off parameters.

From the examples presented above, one sees that the shell structure influences the low energy behavior of the level density in a rather complicated way. At high excitation energy the effect of the shells on the level density becomes somewhat simpler. It was pointed out previously that, for a periodic single particle spectrum which on the average has constant density, the high energy limit for the entropy is: $S = 2\sqrt{a(E - \Delta E)}$. In this limit the shell effect takes the form of a constant energy shift. This is not true for the general case of an arbitrary set of single particle levels and it is instructive to observe the behavior of the effective shift ΔE for different excitation energies. The results of a calculation (57) based on a set of Nilsson single particle levels is shown for the nucleus ^{124}Pd in Figure 3. This nucleus is four protons removed from the fifty proton shell and four neutrons removed from the 82 neutron shell. The quantities ΔE and the proton chemical potential are plotted versus the excitation energy. The chemical potential has the property of

moving towards the region of low single particle level density. This rule is very useful in understanding the behavior of the system as the excitation energy increases. The initial averaging over the shell structure results in a drifting of the chemical potential into the fifty proton shell gap. When the shell structure is washed out the chemical potential continues to decrease because it senses the smoothly decreasing behavior of the single particle level density. This slow decrease of the chemical potential with increasing excitation energy is responsible for the slow decrease of ΔE with energy even after the shell structure is washed out.

System of Interacting Fermions.--

A realistic treatment of the statistical nuclear properties requires the introduction of the residual interactions. This can be done in a rather simple way by means of the pairing interaction: in this case the problem reduces to the choice of the BCS quasi particles (58) as the basic non-interacting fermions (30-32,43-49). Very recently a more fundamental attempt has been made to include realistic residual interactions in level densities in the very same spirit as they are introduced in spectroscopical studies (59-61). The

apparently inextricable problem associated with many interacting particles in a large spectroscopical space can be overcome by the statistical simplifications associated with the central limit theorem. Since a detailed presentation of this method goes beyond the scope of this work only a brief description will be made of the simplest residual interaction, namely the pairing correlation.

The Hamiltonian including the pairing interaction can be expressed in its second quantization form:

$$H = \sum_{\pm K} \varepsilon_K \, a_K^\dagger \, a_K - G \sum_{KK'} a_{K'}^\dagger, a_{-K'}^\dagger, a_{-K} a_K \quad , \qquad 22.$$

where ε_K are the single particle energy levels, $a_K^\dagger$ and a_K are the creation and annihilation operators and G is the pairing strength. Such a Hamiltonian can be approximately diagonalized by means of the quasi particle transformation described first by Bogoliubov (62). In such a description, the excitations are considered to be independent fermions whose energy is given by:

$$E_K = \sqrt{(\varepsilon_K - \lambda)^2 + \Delta^2} \quad , \qquad 23.$$

where λ is the chemical potential and the quantity Δ or gap parameter is a measure of the pairing correlation. The logarithm of the grand partition function is:

$$\Omega = -\beta \sum (\varepsilon_K - \lambda - E_K) + 2 \sum \ln[1 + \exp(-\beta E_K)] - \beta \frac{\Delta^2}{G} \quad , \quad 24.$$

provided that Δ, λ, β are connected by the following relation:

$$\frac{2}{G} = \sum_K \frac{1}{E_K} \tanh \frac{1}{2} \beta E_K \quad , \qquad 25.$$

which is called the gap equation because it defines the gap parameter Δ. The first integrals of motion and the entropy of the system can be obtained from Ω:

$$N = \sum [1 - \frac{\varepsilon_K - \lambda}{E_K} \tanh \frac{1}{2} \beta E_K] \qquad 26.$$

$$E = \sum \varepsilon_K [1 - \frac{\varepsilon_K \lambda}{E_K} \tanh \frac{1}{2} \beta E_K] - \frac{\Delta^2}{G} \qquad 27.$$

$$S = 2 \sum \ln[1 + \exp(-\beta E_K)] + 2\beta \sum \frac{E_K}{1 + \exp(\beta E_K)} \qquad 28.$$

The gap equation describes the dependence of Δ on the temperature T. The gap parameter Δ decreases with increasing temperature and vanishes at a critical temperature t_c which, for the uniform model, is:

$$t_c = \frac{2\Delta}{3.5} \quad .$$

Above this temperature the pairing correlation disappears and the system reverts to the uncorrelated condition. This is caused by the blocking effect of the quasi particles; the levels occupied by them become unavailable to the pairing interaction which decreases and eventually disappears. The only recollection of the pairing interaction is associated to a shift of the effective ground state:

$$E_P - E_U = \frac{1}{2} g \Delta_o^2 \quad . \qquad 29.$$

A complete presentation of this formalism is available in References 47 and 49. The behavior of a paired system restricted to a fixed angular momentum can also be described (46,47). Angular momentum, as excitation energy, tends to destroy pairing. At zero temperature, the dependence of the gap parameter Δ upon angular momentum is given by the relation:

$$\frac{\Delta}{\Delta_o} = \left(1 - \frac{M}{M_c}\right)^{1/2} \quad , \qquad 30.$$

where $M_c = g \Delta m$. The quantity M_c is called the critical angular momentum because for higher angular momenta the pairing correlation disappears.

The combined effect of angular momentum and temperature on the gap parameter can be observed in Figure 4 where the lines of equal Δ are projected in the T, M

plane. A very interesting effect called thermally assisted pairing correlation can be observed for angular momenta larger than zero but less than the critical angular momentum. An initial increase in temperature actually increases the pairing correlation instead of decreasing it. Furthermore for angular momenta somewhat higher than the critical value, an increase of temperature produces the onset of the pairing correlation. The cause of such peculiar phenomenon is the following. At low temperature the quasi particles, necessary for the generation of angular momentum are tightly packed around the chemical potential, blocking the levels most relevant to the pairing interaction. An increase in temperature spreads the quasi particles away from the chemical potential thus decreasing the overall blocking. A further increase in temperature generates more and more quasi particles until the pairing correlation breaks down.

Inclusion of Collective Degrees of Freedom.--

In the formalisms described so far, no specific account has been taken for the effect of the collective degrees of freedom. It has been shown that shell effects tend to disappear with increasing excitation energy. The nuclear deformation is itself a shell effect: therefore it is important to know how

the deformation changes with excitation energy. Assuming that the collective degrees of freedom are statistically coupled to the internal degrees of freedom, an excited nucleus is expected to be characterized by a distribution of deformations. The probability of deformation can be calculated within the assumptions listed above and can be expressed as follows (48,49):

$$P(E,\varepsilon) = \frac{\sqrt{2M\, m_\varepsilon}}{h}\; A'^{-1/2}\; \omega(E_T,\varepsilon) \quad , \qquad 31.$$

where ε is the deformation parameter, h is the Planck's constant, m_ε is the inertial parameter associated to the collective motion, $\omega(E_T,\varepsilon)$ is the state density of the nucleus calculated at the deformation ε and at an excitation energy $E_T = E - V(\varepsilon)$, $V(\varepsilon)$ being the potential energy at the deformation ε. The quantity A' is defined as:

$$A' = \left.\frac{d\ln\omega(x)}{dx}\right|_{x = E_T} .$$

An example of "ab initio" calculations of the deformation probabilities based on the Nilsson diagram and the BCS Hamiltonian is shown in Figure 5b. These deformation probabilities must be compared with the potential energy curve vs. deformation shown in Figure 5a. It can be observed that at low

excitation energies, the deformation probability closely reflects the details of the potential energy. However as the excitation energy increases, the structure in the deformation probability is gradually smoothed out until, at sufficiently large energy, the deformation probability peaks at sphericity, with a large dispersion. At these energies the deformation probabilities reflect more the trend of the liquid drop potential energy than the actual potential energy which is modulated by the shell effects. This example shows dramatically how the washing out of the shell effect takes place with increasing excitation energy.

EXPERIMENTAL SOURCES OF INFORMATION ON LEVEL DENSITIES

Experimental data on nuclear level densities has generally been analyzed with a theoretical expression based on the equidistant model (see Equation (14)). Although an expression of this type is usually referred to as a Fermi gas level density, this is not strictly true since the equidistant model as discussed earlier represents only a zeroth order approximation to the single particle density of a Fermi gas. The level density parameters $\underline{a}$ (defined after Equation (13)) and $\underline{\Delta}$ (defined below) vary with A but for a particular nucleus are assumed to be constants independent of excitation energy. The quantity $\underline{\Delta}$ is an energy shift which defines a fictive ground state with respect to the actual ground state. Hence, the quantity E in Equation (14) is replaced with an effective energy $E^*=E-\Delta$. In most analyses of data Δ is assumed to be a pairing energy (63,64,19) (see section on Neutron Resonances). However, in more recent analyses of data, $\underline{\Delta}$ is treated as an adjustable parameter including the effects of nuclear shells as well as pairing (42,65-68).

If one adopts the point of view that $\underline{a}$ and $\underline{\Delta}$ are adjustable parameters, it is sometimes possible in limited regions of excitation energy to approximate with good accuracy level densities associated with non-uniform single particle structures with eq. 14 where $\underline{a}$ and $\underline{\Delta}$ are independent of excitation energy. Such a procedure usually fails, however, near major closed shells where a simple constant temperature formula

$$\rho(E) = \text{const. } \exp(E/T) \qquad 32.$$

is often better (42,69,70). It must be emphasized that these simple forms of the level density are approximations which may not reproduce very well the level density of a nucleus which has marked structure in its single particle levels. Even so, the present state of experimental data is such that essentially all analyses have been performed with level density formulas which contain energy independent parameters.

The third level density parameter determined from experimental data is the spin cutoff parameter σ^2 which characterizes the angular momentum distribution of the level density. Information on this parameter will be discussed in a later section.

Neutron Resonances

Neutron resonance data contribute the most extensive source of information on nuclear level densities. In this type of experiment, the nuclear energy levels are observed at an energy just exceeding the neutron binding energy and the number of levels are obtained by counting the resonances in a particular neutron energy interval. It is necessary in such experiments that the width Γ of each level be less than the level spacing D and that the experimental resolution is good enough to resolve individual levels. The levels excited by neutron-resonance spectroscopy have narrowly selected values of angular momentum I and parity π quantum numbers.

Level spacing information has been obtained from slow-neutron resonance (s-wave) data for about 200 nuclei. Average resonance spacings $\langle D_I(E) \rangle$ and references to the experimental data are given in several compilations (16,18,19,71-74). One of the important aspects of this method is its applicability to the entire range of A values across the whole periodic table. Hence, it is possible to investigate trends

and systematics of the nuclear level density as a function of A. Although the technique of neutron resonance spectroscopy is an extremely important one in terms of level density information, it suffers from a number of sources of experimental error. First of all, the strengths of resonances of a particular spin and parity vary greatly from one resonance to another. Hence, from cross section measurements over a given energy region, one cannot be certain that all the s-wave resonances have been detected. Secondly, if positive means of identification have not been used, one cannot be certain that some of the resonances detected are not of p-wave character. The probability of observing p-wave resonances with low energy neutrons is greater for light nuclei and regions of A where a maximum exists in the p-wave strength function. Fortunately, the above two errors are to a certain extent compensatory. Finite instrumental resolution may lead to an underestimate of the number of resonances in cases where close-lying resonances are unresolved.

For a target with zero spin, s-wave neutron capture

gives the density of levels of a single angular momentum and parity $1/2^+$. If the angular momentum dependence of the level density is given by Equation (14), the total level density $\rho(E)$ is related to the average spacing between $1/2^+$ levels $\langle D_{1/2^+} \rangle$ by,

$$\rho(E) = 2\sigma^2/\langle D_{1/2^+} \rangle \qquad 33.$$

Authors (16-19,29,73,75,76) have traditionally analyzed neutron resonance data with level density formulas of the type given by Equation (14). A recent compilation (29) of the level density parameter a as a function of atomic mass A is shown in Figure (6). Each level density parameter in Figure (6) depends upon a knowledge of two other parameters, σ and Δ. The spin cutoff parameter in this analysis was calculated from Equation (16) where $g\langle m^2 \rangle$ is assumed equal to the rigid-body moment of inertia $\mathcal{I}/\hbar^2$. The energy shift Δ was assumed equal to the pairing energy values of Gilbert and Cameron (19).

One observes from Figure (6) that there is an overall increase of a with increasing values of A. However, marked deviations occur from the straight line where a=A/8, especially

for A values near closed shells. For example, in the vicinity of the Z=82 and N=126 shells, $\underline{a}$ values are more than a factor of two smaller than those of nearby nuclei. Such irregularities are associated with shell structure of the single particle spectrum near the Fermi energy and have been discussed by a number of authors (16,17,19,29,72,73,75,76). Gilbert and Cameron (19) have also applied a composite nuclear-level density formula with shell corrections to the neutron resonance data.

There are also other difficulties in the determination of level densities by the neutron resonance technique. When the average spacing is large and few resonances are observed, there is a source of uncertainty of a statistical nature that is due to the irregularity in spacing between individual levels (72). The calculation of the total level density from the density of levels of a single spin and parity requires a knowledge of both the angular momentum and parity dependence of the level density. At the neutron binding energy, calculations of the ratio of positive to negative

parity levels for some nuclei show that this quantity varies considerably from unity (44). Fluctuations in the density of levels of a particular J and π are expected to occur due to nuclear shell structure. Hence, for such nuclei the density of $1/2^+$ levels at the neutron binding energy may not give a true representation of the total level density. Capture of s-wave neutrons in targets of non-zero spin leads to the excitation of levels of two classes with angular momenta differing by one unit. This makes the interpretation of such data more difficult.

The neutron resonance data gives a measure of the density of levels for a single parity and one or two values of angular momentum in a single energy region just above the neutron binding energy. The level density parameters extracted from these data by Equations (33) and (14) do not necessarily have general applicability, especially in regions of higher and lower excitation energy. This subject will be discussed in later sections.

Charged-particle Resonances

Information on the density of levels of restricted angular momentum is obtained from charged particle capture resonances in the same way as described for neutron capture resonances. In addition to the requirement that $\Gamma<D$, the charged-particle resonance data are restricted to light and medium nuclei due to the Coulomb barrier. One of the heavier targets studied by this technique is ^{64}Ni. In this case, for example, the capture of 3.11 to 3.28 MeV protons on a target of ^{64}Ni has led to the identification of a number of s-wave and p-wave resonances (77) in the compound nucleus ^{65}Cu. From the density of observed resonances ρ_{res}, the total density of levels $\rho(E)$ is calculated from the relation

$$\rho_{res} = \rho(E) \sum_{I,\pi} [(2I+1)/4\sigma^2]\exp[-(I+1/2)^2/2\sigma^2] \qquad 34.$$

by summing over the spins and parities of the resonances. In some cases considerable error may arise due to the assumption which is made about the ℓ waves contributing to the total number of resonances. The other uncertainties in the determination of the level density from charged-particle

capture resonances are similar to those discussed previously for neutron capture resonances.

The study of charged-particle resonances gives level density information for a number of nuclei which cannot be studied by neutron resonance spectroscopy. A compilation of such data for a number of light nuclei has been published by Endt and van der Leun (78). Some nuclei have been studied by more than one reaction. For example, levels in the compound nucleus ^{28}Si have been observed as resonances in the $^{27}Al(p,\gamma)$, $^{24}Mg(\alpha,\gamma)$ and $^{27}Al(p,\alpha)$ reactions. This data has been analyzed to give the total number of levels in ^{28}Si in the vicinity of 12.5 MeV (67).

Recently, a high resolution technique has been developed and used in the measurement of proton excitation functions for even-even targets in the mass region $40 \leq A \leq 64$ (77,79-86). With protons of energy between 2 and 3 MeV, a resolution of approximately 400 eV has been obtained for thin solid targets. Spins, parities, total and partial widths of the compound states are determined. For even-even targets, s-wave proton

capture excites $1/2^+$ compound levels. Level densities in the compound nucleus ($E=B_p+E_p$) based on the $1/2^+$ resonances are consistent with other level density data (87). One of the unique features exploited with this technique is the study of fine structure of analogue states. Since the analogue state, $T_>$, mixes to some degree with the $T_<$ levels of the excited compound nucleus, the number of resonances one observes is a function of the density of $T_<$ levels which have the same spin and parity as the analogue state. Since the proton bombarding energy is low, few p-wave resonances are observed for nuclei in the mass range 40 to 64 except at energies in the vicinity of an analogue state. In the energy region of an analogue state, the strength of the $T_>$ state is shared with the $T_<$ background states. The widths of the $T_<$ levels are sufficiently enhanced to make a number of them experimentally observable. Even so, an examination of the p-wave resonances ($1/2^-$ and $3/2^-$ levels) in the vicinity of an analogue state indicate that there are too few such resonances relative to the number of s-wave resonances ($1/2^+$ levels). If all the

$1/2^+$ and $1/2^-$ levels were excited as s- and p-wave resonances, it would be possible to measure directly the positive to negative parity ratio of these levels.

Inelastic Scattering and Nuclear Reactions to Resolved Levels

Level density information from neutron and charged-particle resonances as described in the above sections is limited to energies exceeding the appropriate binding energy. These levels are in the compound nucleus and they are separable due to high resolution experimental techniques. A large number of levels have been studied also in residual nuclei at lower energies by excitation through inelastic scattering and a variety of other nuclear reactions. The resolution obtained in these experiments is orders of magnitude poorer than that achieved with s-wave neutron spectroscopy. A typical resolution obtained with a Van de Graaff acclerator and a magnetic spectrograph is of the order of 10 keV for energetic charged particles. With such equipment, it is possible to study isolated levels up to an excitation energy of approximately 5 to 6 MeV for a nucleus with atomic mass

around 60. The resolution obtainable by these techniques may be improved to approximately 1 keV in the near future (88) and this will make this technique more attractive.

Typical nuclear reactions which have been employed to study levels at low energies are the (p,p'), (n,n'), (α,α') and (p,α) reactions. Although a number of levels have been studied with (d,p) and (d,t) reactions, these and other similar direct reactions are more likely not to excite all the nuclear levels. If this technique is to be used for accurate level density information, one must be assured that levels of all angular momenta are excited. For compound nucleus reactions, the relative cross sections for populating levels of different I can be calculated. Results of such statistical calculations are discussed in the literature (89) for the ^{56}Fe(p,p') and ^{59}Co(p,α) reactions for 11 MeV proton bombarding energy. The relative intensities for exciting low and high angular momentum levels by the two reactions are very different. The relative cross section for exciting high spin states such as I=8 states is still large for the ^{59}Co(p,α) reaction. On the basis of the spin dependent

level density given by Equation (14), and a spin cutoff factor of 3.7 for ^{56}Fe (90), one calculates that only a very small percentage of the levels have I>8. Hence, by choosing the appropriate reactions it is possible to excite essentially all the nuclear levels. The levels in the $^{56}Fe(p,p')$ reaction (89) above 3 MeV of excitation energy are shown in Figure (7). Levels 8 and 11 are very weakly excited, however, these levels are more strongly excited in the $^{59}Co(p,\alpha)$ reaction and must have $I \geq 6$.

With this method, a second question must be raised about the fraction of levels which lie so near another level that the pair is unresolved due to the finite experimental resolution. It is true that at sufficiently high excitation energies the levels are unresolved, but how can one estimate the number of unresolved pairs of levels at lower excitation energies? The spacing between adjacent levels having the same spin and parity is distributed relative to the mean spacing according to the Wigner distribution given by (91)

$$P(S/\bar{S}) = (\pi S/2\bar{S}) \exp(-\pi S^2/4\bar{S}^2) \qquad 35.$$

where S is the spacing and $\overline{S}$ the average spacing between levels. This distribution has a deficiency of small spacings. If on the other hand, levels occur in a completely random way, one obtains an exponential distribution given by,

$$P(S/\overline{S}) = \exp(-S/\overline{S}) \qquad 36.$$

which has a maximum value for $(S/\overline{S})=0$. In the present case where we are dealing with levels of mixed spin and parity, Wigner proposed that these levels of different spin and/or parity are not in any way correlated in position. The resulting distribution of spacings from a sequence of levels which is a superposition of sets of different spin and/or parity has a shape intermediate between the Wigner distribution and the exponential distribution. The theoretical distribution of spacing resulting from the random superposition of a number of unrelated sequences, each of which has a Wigner distribution, has been derived by Rosenzweig and Porter (92). For a spin dependent level density given by Equation (14) and levels of both parities, the distribution of spacing approaches the exponential distribution even for rather small values of

σ (93). An analysis of the experimental spacing distribution for 622 levels with $\overline{S} \geq 30$ keV has been made (93) for levels in nuclei ^{36}Ar (94), ^{38}Ar (94), ^{40}Ca (95), ^{45}Sc (96), ^{47}V (97), ^{49}V (97), ^{50}Cr (98), ^{51}V (99), ^{52}Cr (89,98), ^{53}Cr (98), ^{54}Cr (98), ^{54}Fe (100), ^{55}Mn (89), ^{56}Fe (101,102), ^{57}Fe (103), ^{58}Fe (103), ^{59}Co (101), and ^{66}Zn (89). The experimental data fit an exponential spacing distribution as shown in Figure (8). If the experimental resolution is known, it is possible to use the exponential spacing distribution law to correct the experimental level density for missed levels due to unresolved levels with spacings less than the experimental resolution (89, 104). At 5 to 6 MeV, the correction for a nucleus with A=60 may approach 50%.

Compilations of the energies of nuclear levels and in some cases information on their spins and parities are published for a number of nuclei (78,105,106). The use of level density counting information at low energy in conjunction with particle capture resonance data gives a more critical test of level density formulas. In the calculation of the values of

$\underline{a}$ plotted in Figure 6), the ground state of the odd-odd nuclei served as the fictive ground state of the Fermi gas. The excitation energies of the odd A and even-even A nuclei were reduced (29) by the appropriate pairing energy of Gilbert and Cameron (19). Such a formulation of the level density is inadequate to fit both the low excitation energy (level counting) and particle capture resonance data. A better fit to all the data is obtained if the level density parameter $\underline{a}$ and the energy shift Δ, which defines a fictive ground state with respect to the actual ground state, are treated as adjustable parameters. Except in the neighborhood of closed shells, the experimental level densities are best fitted with an energy shift corresponding to a fictive ground state of the Fermi gas being located between the actual ground states of the even-even and odd A nuclei (65-68,107). This model has been referred to as a back-shifted Fermi gas model (65,67). Values of effective level density parameters $\underline{a}_{eff}$ and $\underline{\Delta}_{eff}$ have been determined from state density calculations (42) which use Nilsson single particle states by fitting the

theoretical level densities with a formula such as Equation (14). Such calculations give effective values of $\underline{a}$ and $\underline{\Delta}$ in reasonable agreement with the experimentally determined values (42).

Spectrum of Evaporated Particles

The energy and angular distribution of particles emitted from a compound nucleus in a nuclear reaction is given by (108-112),

$$\frac{d^2\sigma_{ab}(\varepsilon_b)}{d\varepsilon_b d\Omega_b} = \sum_{\substack{L=0 \\ \text{even}}}^{\infty} B_L(\varepsilon_b)\, P_L(\cos\theta) \qquad 37.$$

The function $B_L(\varepsilon_b)$ is given by

$$B_L(\varepsilon_b) = \frac{(2I_a+1)^{-1}(2i_a+1)^{-1}\, k_a^{-2}}{4} \sum_{S_a,S_b,I_b,\ell_a,\ell_b,I}$$

$$\frac{(-)^{S_a-S_b} T_a^{\ell_a}(\varepsilon_a)\; T_b^{\ell_b}(\varepsilon_b) Z(\ell_a I \ell_a I; S_a L) Z(\ell_b I \ell_b I; S_b L) \rho(E_b, I_b)}{G(I)} \qquad 38.$$

and G(J) is given

$$G(I) = \sum_{b'} \int_0^{E_{b'max}} dE_{b'} \sum_{\ell_{b'}=0}^{\infty} T_{b'}^{\ell_{b'}}(\varepsilon_{b'}) \sum_{S_{b'}=|I-\ell_{b'}|}^{I+\ell_{b'}} \sum_{I_{b'}=|S_{b'}-i_{b'}|}^{S_{b'}+i_{b'}} \rho_b(E_{b'}, I_{b'}) \qquad 39.$$

The quantities I_a, i_a, I, I_b, and i_b are the spins of the target,

projectile, compound nucleus, residual nucleus, and the emitted particle, respectively; S_a and S_b are the channel spins in the incident and outgoing channels, respectively; ℓ_a and ℓ_b are the orbital angular momenta of the incident and outgoing particles, respectively; k_a is the wave number of the incident particles; $P_L(\cos\theta)$ is the Legendre polynomial of the order L; $T_a^{\ell_a}(\varepsilon_a)$ and $T_b^{\ell_b}(\varepsilon_b)$ are the transmission coefficients for the projectile and emitted particle, respectively, with the channel energies ε_a and ε_b (the channel energy ε is defined as the sum of the center of mass kinetic energies of the emitted particle and recoil nucleus); $Z(\ell_a I \ell_a I; S_a L)$ and $Z(\ell_b I \ell_b I; S_b L)$ are the so-called Z coefficients and are defined as the product of the Racah coefficient W, and the Clebsch-Gordan coefficient $(\ell\ell 00; L0)$ as

$$Z(\ell I \ell I; SL) = (2\ell+1)(2I+1)(\ell\ell 00|L0)W(\ell I \ell I; SL) \qquad 40.$$

One of the properties of the Z coefficients is that they vanish unless $2\ell+L$ is even. This means that L must be even. This property has the consequence that only the even order Legendre Polynomials $P_L(\cos\theta)$ are present, i.e. the angular

distribution is symmetric around 90° in the center of mass system. The quantity $\rho_b(E_b,I_b)$ is the energy and spin dependent level density of the residual nucleus formed by the emission of particles b with channel energy ε_b; and the primed quantity, b', refers to the different types of emitted particles. The sums in the numerator can be performed independently with respect to the quantum numbers ℓ_a,ℓ_b,I and I_b since the Z coefficients vanish for combinations of the quantum numbers which violate the conservation of angular momentum.

The energy dependent differential cross section is obtained by integrating Equation (37) over all angles. Only the term with L=0 contributes to the energy dependent differential cross section since the higher order Legendre polynomials vanish when integrated over the solid angle.

The product of the Z coefficients

reduces to a very simple form since for L=0 the Clebsch-Gordan and the Racah coefficients have the form

$$(\ell\ell 00|00) = (-)^{\ell}/\sqrt{2\ell+1}$$

41.

$$W(\ell I\ell I;S0) = (-)^{S-\ell-I}/\sqrt{(2\ell+1)(2I+1)}$$

Noting the fact that ℓ_a, ℓ_b and L must obey the triangular relationship and that integration of Equation (37) over $d\Omega$ introduces a factor of 4π, the energy distribution of the evaporated particles is given by (87,108,113)

$$\frac{d\sigma_{ab}(\epsilon_b)}{d\epsilon_b} = \frac{\pi k_a^{-2}}{(2I_a+1)(2i_a+1)} \sum_{S_a=|I_a-i_a|}^{I_a+i_a} \sum_{\ell_a=0}^{\infty} T_a^{\ell_a}(\epsilon_a) \cdot$$

$$\sum_{I=|\ell_a-S_a|}^{\ell_a+S_a} \frac{(2I+1)}{G(I)} \sum_{\ell_b=0}^{\infty} T_b^{\ell_b}(\epsilon_b) \sum_{S_b=|I-\ell_b|}^{I+\ell_b} \sum_{I_b=|S_b-i_b|}^{S_b+i_b} \rho_b(E_b, I_b) \qquad 42.$$

If one assumes that the spin dependent level density has a $(2I+1)$ dependence, $\rho(E_b,I_b) = (2I_b+1)\rho(E_b,I_b=0)$, then Equation (42) reduces to

$$\frac{d\sigma_{ab}(\epsilon_b)}{d\epsilon_b} = K\ \sigma_b(\epsilon_b)\ \epsilon_b\ \rho_b(E_b,I_b=0) \qquad 43.$$

Substitution of the spin dependent level density given by Equation (14) for zero spin levels into Equation (43) gives

$$\frac{d\sigma_{ab}(\epsilon_b)}{d\epsilon_b} = K'\sigma_b(\epsilon_b)\ \epsilon_b\ (E_b+t_b-\Delta_b)^{-2}\exp\{2[a(E_b-\Delta_b)]^{1/2}\} \qquad 44.$$

where K' is a new constant for a particular bombarding energy.

From Equation (44), the value of the Fermi gas constant $\underline{a}$ can be determined from the slope of the straight line obtained from a plot of

$$\ln\{[d\sigma_{ab}(\varepsilon_b)/d\varepsilon_b](E_b+t_b-\Delta_b)^n/\varepsilon_b\sigma_b(\varepsilon_b)\} \text{ vs. } (E_b-\Delta_b)^{1/2} \qquad 45.$$

where the parameter n=2. If, on the other hand, the constant temperature level density is substituted into Equation (43), the constant temperature T_b may be obtained from the slope of the straight line given by a plot of

$$\ln\{[d\sigma_{ab}(\varepsilon_b)/d\varepsilon_b](E_b+t_b-\Delta_b)^m/\varepsilon_b\ \sigma_b(\varepsilon_b)\} \text{ vs. } E_b-\Delta_b \qquad 46.$$

where the parameter m=1/2. The latter plot can equally well be made as a function of E_b.

A large number of particle spectra including those from the (n,n'), (p,n), (α,n), (n,p), (p,p'), (p,α), (n,α), (p,α) and (α,α') reactions have been analyzed to determine information on level densities (69,70,87,107,114-171). Most of the spectra have been analyzed with Equations (45) and (46). The values of n used in Equation (45) have included 5/4, 3/2 and 2 corresponding to the use of the state density, the level density and the level density of a particular angular momentum,

respectively. In addition, some authors have set n=0 which assumes that the preexponential term in the level density formula is insignificant in terms of the overall exponential dependence of the level density on E.

In order to illustrate the dependence of the parameter a on the value of n when spectra are analyzed with the Weisskopf type formula given by Equation (45), we show such analyses of theoretical spectra (87). The $^{63}Cu(p,p')^{63}Cu$ and $^{60}Ni(\alpha,\alpha')^{60}Ni$ spectra were calculated with the exact statistical theory including angular momentum given by Equation (37), employing level density parameters a=6.8 MeV^{-1}, Δ=-0.5 MeV and 5.8 MeV^{-1}, Δ=0.5 MeV, respectively (and rigid-body moments of inertia). As shown in Figure (9), the approximate slope technique of Equation (45) gives a different value of a for each value of n. The value of n needed to reproduce the input value of a depends on the reaction type, with smaller values of n required for (α,α') reactions than for (p,p') reactions. The value of n needed to reproduce the actual value of a depends on reaction angle also, especially

for reactions where large I values are excited.

Level density parameters in the literature which are deduced from the conventional analysis of spectra (Equation (45)) with values of n ranging from 0 to 2 are subject to sizeable errors. The errors in $\underline{a}$ are up to 50% depending on the value of n. The slope technique requires also a knowledge of $\underline{\Delta}$ and this leads to further ambiguity in the derived value of $\underline{a}$. The experimental spectral data are usually not sufficiently accurate to distinguish between a constant temperature (Equation (32)) and Fermi gas (Equation (15)) type of level density. In some cases, the values of $\underline{a}$ derived from (n,n') spectra are a factor of two different from those derived by other methods. These discrepancies appear to be related to experimental difficulties and the methods of data analysis.

There is evidence for some nuclei, however, that the level density is increasing with energy in a way predicted by the Fermi gas model. For example, the neutron spectra from the $^{103}Rh(p,n)^{103}Pd$ reaction (133) show an increase in

temperature with increasing bombarding energy. If the energy range of the emitted neutrons is kept fixed with increasing bombarding energy, the spectra sample regions of increasing energy in the residual nucleus. The results of theoretical spectra calculated with Equation (37) and analyzed with the approximate Equation (46) are shown in Figure (10). The variation of temperature with bombarding energy is in excellent agreement with experimental results analyzed (52) with the same approximate Equation (46) and supports an energy dependence similar to that of the Fermi gas level density (Equation (15)).

Evidence exists also in support of a constant temperature type level density at low excitation energy, especially for nuclei in the vicinity of closed shells (42,52,69,70).

Several analyses have been made on portions of evaporation spectra corresponding always to the same range of energy in the residual nucleus for different incident energies. In this case, a variation in the level density parameter with bombarding energy is not expected and implies some error in the analysis procedure. Bodansky (151) has reviewed some

of the explanations for the observed increase in temperature with incident energy. As the incident energy is increased, there is an increased probability of particle emission before thermal equilibrium is established or preequilibrium emission (172-175). This leads to a higher percentage of high energy particles in such spectra. Secondly, observed cross sections depend not only on the level density but also on the inverse cross sections which may be in error. Thirdly, the conventional analysis with the Weisskopf formula produces the effect of a higher temperature because the angular momentum is ignored. In some cases at least, the observed variation of level density parameters with bombarding energy cannot be entirely due to the neglect of angular momentum, and must be due to one or both of the other two factors.

As already indicated, erroneous values of the level density parameter a may be obtained when nuclear evaporation spectra are analyzed with the conventional formalism that does not explicitly take account of the spin dependent level density. The apparent value of a from a reaction spectrum

depends both on the mode of formation of the compound nucleus and the type of particle emitted. This makes it difficult to extract a meaningful value of $\underline{a}$ from a single evaporation spectrum with the conventional theory. Recently, the level densities of several nuclei with mass around A=60 have been studied by measuring spectra from several suitably chosen reactions which populate the same residual nucleus (87,160, 161). Such studies give a more stringent test of the validity of the various approximate formulas and show the necessity in a number of cases of employing the exact statistical theory with angular momentum in evaluating the level density parameter. Comparison of (p,α), (α,α'), and (α,p) spectra give the same level density parameter whereas the (p,p') spectrum leads to a smaller value of $\underline{a}$ (87,160). This may be understood in terms of a contribution of pre-equilibrium protons in the (p,p') evaporation spectrum leading to a harder spectrum and a smaller value of $\underline{a}$.

In most analyses of reaction spectra by the conventional slope technique one obtains only the level density parameter

a. Occasionally, the absolute level density is obtained by normalizing the level density in a particular low energy range to the known number of levels in this energy region determined by high-resolution magnetic spectroscopy (165).

Excitation Functions of Isolated Levels

Absolute cross sections for formation of isolated residual levels in compound nucleus reactions can be used to determine nuclear level densities (65). This was first pointed out by Ericson (6). Since the cross section for formation of any particular level (or levels) is governed by the competition of decay probability through this selected reaction channel (or channels) to that for all other channels, the number of competing channels can be determined from the cross section of a single channel. Measurements of the absolute cross sections for isolated final levels as a function of bombarding energy have been used to determine the energy dependence and absolute values of the level densities of the residual nuclei (65). In the limiting case where one type of exit particle dominates (usually the neutron channels), the

level density of a single nucleus is obtained.

According to the statistical theory of nuclear reactions, the differential cross section for a reaction leading to a final state with angular momentum I_B, parity π_B and excitation energy E_B in the residual nucleus B, can be expressed by Equations (37) to (39) where the level density in the numerator of Equation (38) is replaced by a single level. The excitation function of the single level (or levels) is fitted with different choices of the level density parameters for the other exit channels in order to give the best agreement between experiment and theory. In order to fit both the absolute value of the cross section and its energy dependence with a Fermi gas type level density, both $\underline{a}$ and $\underline{\Delta}$ need be adjusted (65). Hence, this technique has some intrinsic advantages and gives an absolute measure of the level density. On the other hand, the technique suffers from the exponentially decreasing cross section with energy of a single level and the possible admixture of direct reaction particles. Improvement in statistical accuracy can be attained by examining

the energy dependence of the cross section of many final levels (143,144). However, other uncertainties in the analysis offset the advantage gained by better statistics.

Ericson Fluctuation Widths

A number of nuclear reaction cross sections have been measured with good energy resolution at a compound nucleus excitation energy of approximately 20 MeV. These cross sections fluctuate markedly as a function of projectile energy and have been extensively analyzed in terms of statistical theory. For the energy region where the average level width Γ is larger than the average spacing D between compound nuclear levels, Γ is obtainable from correlation functions of the fluctuating cross sections. This average width Γ of the compound states is related by statistical theory to a sum of the partial widths of all the exit channels,

$$\Gamma_I(E) = (D_{I,\pi}(E)/2\pi)\ G(I) \qquad 47.$$

where G(I) is defined by Equation (39). If the width Γ of the compound nuclear states is known from cross section fluctuation measurements and information on the exit channels is known from

other measurements, the level density of the compound nucleus at a high excitation energy of approximately 20 MeV is obtained (65,66,107,176,177).

Substitution of Equation (47) into Equations (37) and (38) and making some simplifying assumptions gives,

$$\frac{d\sigma_{ab}}{d\Omega}(I_B,\pi_B,E_B,\theta)\,\frac{\Gamma(E)}{D_0(E)} = \frac{k_a^{-2}}{4\pi(2I_A+1)(2I_a+1)}$$

$$\sum_{S_1,l_1,S_2,l_2,I,L} \frac{\delta_n{}^m(-1)^{S_2-S_1}T_{al_1}(\varepsilon_1)T_{bl_2}(\varepsilon_2)Z_1Z_2P_L(\cos\theta)}{(2I+1)\exp[-I(I+1)/2\sigma_C{}^2]} \qquad 48.$$

where $D_{0,\pi}(E_C)$ is the spacing of zero spin levels of one parity and σ_C is the spin cutoff factor of the compound nucleus at excitation E_C. The width $\Gamma(E)$ is now defined as a weighted average over the width $\Gamma_I(E_C)$ of the various compound spin states. The above weighting factors are dependent on excitation energy, angle θ, and the spin and parity of the final state. However, the influence of these factors on $\Gamma(E)$ is rather weak and Equation (48) is quite a good approximation. The right-hand side of this equation depends on the quantum numbers I_B and π_B of the populated level in the residual

nucleus, transmission coefficients of the entrance and exit channels and the spin cutoff factor σ_C of the compound nucleus. As information exists on all these quantities, it is possible to evaluate the right-hand side of Equation (48). The quantity $\Gamma(E_C)/D_O(E_C)$ can then be computed as a function of excitation energy E_C if measurements of $d\sigma_{ab}/d\Omega(I_B,\pi_B,E_B,\theta)$ are available. Values of Γ/D_O for the compound nuclei ^{56}Fe and ^{60}Ni are plotted in the literature (65) as a function of energy for both rigid- and half-rigid-body moments of inertia. The quantities $D_O(E_C)$ and $\rho(E)_C$ can be calculated from the values of $\Gamma(E_C)/D_O(E_C)$ if independent knowledge of the level width $\Gamma(E_C)$ as a function of energy is available.

Level density results from this technique for excitation energies near 20 MeV are published (65, 66, 176, 177) for several nuclei. An example of such results for ^{60}Ni is shown in Figure (11). Presently, this is the only method which gives information on the level density at such high excitation energies. References to the original literature on fluctuation widths are available in review articles (178-180).

Compound Nucleus Lifetime and Level Density from the Blocking Effect

Several measurements have been reported of the mean compound nucleus lifetimes based on the blocking effect of inelastic charged particles in single crystals (181-183). This technique offers a method of determining lifetimes in the neighborhood of 10^{-17} seconds. If a small number of final states are excited with known yields, it is possible to calculate the density of compound levels from such lifetime measurements with the Hauser-Feshbach (110) statistical theory. Furthermore, it has been observed that the final state spins affect the effective lifetimes in a manner which can be understood on the basis of selective contributions by the various compound nuclear angular momenta (184).

Spin Distribution of the Nuclear Level Density

A property of the nuclear level density which is of great general interest is its spin dependence. The angular momentum dependence is explicitly contained in Equations (12) and (14) through the quantity σ^2, which is called the spin cutoff

parameter. The simple form of the spin dependent level density given in these equations is expected to fail for large values of the angular momentum. Hence, the experimental data discussed in this section is limited to systems with relatively small values of angular momentum. Information on the density of levels with very large values of angular momentum may be obtained from Equations (6-8).

Information about σ^2 comes mostly from a) isomer ratio measurements (185,186), b) angular distributions of particles emitted in compound nucleus reactions (112,165,90,170,143), c) analysis of levels of known spin, and d) particle capture to levels of two or more known spin values (187).

The uncertainties involved in the derivation of the spin cutoff factor from experimental data has oftentimes led to results which are subject to large errors. These experimental values of σ^2 have been interpreted in terms of Equation (16), where the moment of inertia is allowed to take on values less than the rigid-body value. Authors in reporting the fractional decrease of the rigid-body moment have used different values

of the radius parameters. For example, a rigid-body moment of inertia computed on the basis of a radius parameter of 1.2 F corresponds to only a 64% rigid-body moment on the basis of a radius parameter of 1.5 F. For $A \leq 10^2$, the experimental σ values are well represented within the large experimental uncertainties by Equation (16) with a rigid-body moment of inertia ($R=1.2\ A^{1/3}F$). The limited amount of information on heavy nuclei indicates that σ remains almost constant for $A>100$ (188). Near $A=200$, the moment of inertia may be reduced in some cases to the extent of half the rigid-body value.

Comparison of the experimental values of σ with theoretical values based on Equation (16) is not too meaningful for particular nuclei in that no account is taken of specific structure in the single particle spectrum. Comparisons of experimental σ values with those predicted for realistic sets of single particle levels are now being made (90). Examples of such comparisons for ^{56}Fe and ^{59}Co are shown in Figure (12). The solid lines are based on Nilsson single particle levels. The dashed line for ^{56}Fe is calculated for a set of single

particle levels based on a potential very similar to that of a Woods-Saxon potential (189). The dot-dashed curves are based on the rigid-body moments of inertia. The experimental data for these nuclei is in good agreement with both theories. However, in evaluation of σ^2 from Equation (10), one observes strong effects due to the particular orbits near the Fermi energy. At low energies for ^{56}Fe the proton contribution (unfilled $f_{7/2}$ orbital in the ground state) to σ^2 is essentially twice the neutron contribution (unfilled $p_{3/2}$ orbital in the ground state). It is obvious that shell structure will influence the spin dependent level density in some regions of A so that the values will deviate markedly from the predictions of Equation (16) based on the rigid-body moment of inertia. For example, experimental measurements on nuclei below lead indicate that σ is approximately 4 ± 1 in the vicinity of the neutron binding energy (a value much smaller than predicted by Equation (16)). Calculations based on various single particle level schemes give similar values for nuclei at and just below the double closed Z=82,

N=126 shell as shown in Figure (2). These calculations do not include pairing which in some cases reduces considerably the value of σ^2. In conclusion, it appears that our present experimental information on the spin dependent level density can be qualitatively understood in terms of nuclear shell structure.

REFERENCES

1. For a discussion on this subject see for instance: Bohr, A. Mottelson, B. 1969. Vol. I-156-181. W. A. Benjamin, Inc., New York, Amsterdam.

2. Bohr, N. 1936. Nature 137:344

3. Bohr, N., Kalckar, F. 1937. Math-fys. Medd. 14 No. 10

4. Weisskopf, V. F. 1937. Phys. Rev. 52:295; 1950 Helv. phys. acta. 23:187; 1953 Proc. Amer. Acad. Arts. Sci. 82:360

5. Weisskopf, V. F., Ewing, D. H. 1940. Phys. Rev. 57:672

6. A very braod review of the subject is available in: Ericson, T. 1960. Advance in Physics 9:425

7. Bethe, H. 1936. Phys. Rev. 50:332; 1937 Rev. Mod. Phys. 9:69; 1938 Phys. Rev. 53:675

8. Van Lier, C., Uhlenbeck, G. 1937. Physica 4:531

9. Lang, J. M., Le Couteur, K. J. 1954. Proc. Phys. Soc. Lond. A67:585

10. Lang, J. M., Le Couteur, K. J. 1959. Nucl. Phys. 14:21

11. Lang, D. W. 1965. Nucl. Phys. 77:545

12. Kanestrøm, I. 1966. Nucl. Phys. 83:380

13. Kanestrøm, I. 1969. Nucl. Phys. A109:625

14. Margenau, H. 1941. Phys Rev. 59:627

15. Bloch, C. 1954. Phys. Rev. 93:1094

16. Newton, T. D. 1956. Can. J. Phys. 34:804

17. Ross, A. A. 1957. Phys. Rev. 108:720

18. Cameron, A. G. W. 1958. Can. J. Phys. 36:1040

19. Gilbert, A., Cameron A. G. W. 1965. Can. J. Phys. 43:1446

20. Rosenzweig, N. 1957. Phys. Rev. 105:950; ibid. 1957 108:817

21. Rosenzweig N., Bollinger, L. M., Lee, L. L. Jr., Schiffer, J. P. 1958. Proceeding of the Second Geneva Conference on Peaceful Uses of Atomic Energy V15 p. 693

22. Ericson, T. 1958. Nucl. Phys. 8:265

23. Rosenzweig, N. 1966. Nuovo Cimento 43:227

24. Kahn, P. B., Rosenzweig, N. 1966. Phys. Letters 22:307

25. Kahn. P. B., Rosenzweig, N. 1969. Phys. Rev. 187:1193

26. Gilbert, A. 1968. Lawrence Radiation Laboratory Report UCRL-18095

27. Gadioli, E., Iori, I., Molho, N., Zetta, L. 1969. Nucl. Phys. A138:321

28. Kahn, P. B., Rosenzweig, N. 1969. J. Math Phys. 10:707

29. Baba, H. 1970. Nucl. Phys. A159:625

30. Sano, M., Yamasaki, S. 1963. Prog. Theor. Phys. 29:397

31. Lang, D. W. 1963. Nucl. Phys. 42:353

32. Vonach, H. K., Vandenbosch, R., Huizenga, J. R. 1964 Nucl. Phys. 60:70

33. Canuto, V., Garcia-Colin, L. S. 1965. Nucl. Phys. 61:177

34. Nemeth, J. 1967. Nucl. Phys. A92:345

35. Motz, L., Feinberg, E. 1938. Phys. Rev. 54:1055

36. Critchfield, C. L., Oleska, S. 1951. Phys. Rev. 83:243

37. Grover, J. R. 1967. Phys. Rev. 157:832

38. Kluge, K. 1967. Nucl. Phys. 51:41

39. Williams, F. C. Jr. 1969. Nucl. Phys. A133:33

40. Moretto, L. G., Stella, R., Caramella-Crespi, V. 1970. Energia Nucleare 17:436

41. Ramamurthy, V. S., Kapoor, S. S., Kataria, S. K. 1970.

Phys. Rev. Letters 25:386

42. Williams, F. C., Jr., Chan, G., Huizenga, J. R. 1972 Nucl. Phys. to be published

43. Decowski, P., Grochulski, W., Marcinkowski, A., Siwek, K., Wilhelmi, Z., 1968. Nucl. Phys. A110:129

44. Hillman, M., Grover, J. R. 1969. Phys. Rev. 185:1303

45. Ignatyuk, A. V., Stavinskii, V. S., Shubin, Yu. 1970 Soviet Journal of Nuclear Physics 11:563

46. Moretto, L. G. 1971. Phys. Letters 35B:379

47. Moretto, L. G. 1972. Nucl. Phys. A185:145

48. Moretto, L. G., Stella, R. 1970. Phys. Letters 32B:558

49. Moretto, L. G. 1972. Nucl. Phys. A182:641

50. See for instance: Fowler, R. H. 1936. Statistical Mechanics, 2nd Edition. Cambridge at the University Press (1966)

51. Huizenga, J. R., Vaz, L., Williams, F. C., Jr., Blann, M.

1970. University of Rochester Report UR-NSRL-28

52. Huizenga, J. R. 1972. Statistical Properties of Nuclei, Edited by J. B. Garg, Plenum Press (New York) p. 425

53. Griffin, J. J. 1966. Phys. Rev. Letters 17:478

54. Ericson, T. 1965. Advances in Physics 9:425

55. Williams, F. C., Jr. 1971. Nucl. Phys. A166:231

56. Bohning, M. 1970. Nucl. Phys. A152:529

57. Moretto, L. G. 1972. Physics Letters 38B:393

58. Bardeen, Cooper, Schrieffer 1957. Phys. Rev. 106:162; ibid. 1957 108:1175

59. Chang, F. S., French, J. B., Thio, T. H. 1971. Ann. Phys. 66:137

60. French, J. B., Chang, F. S. 1972. Statistical Properties of Nuclei, Edited by J. B. Garg, Plenum Press (New York) p. 405

61. Bloch, C. 1972. Statistical Properties of Nuclei, Edited by J. B. Garg, Plenum Press (New York) p. 379

62. Bogoliubov, N. N. 1958. Zh. Experim. i Teor Fiz. 36:7:41; ibid. 1958 34:7:51; 1958 Nuovo Cimento 7:794

63. Hurwitz, H., Bethe, H. A. Phys. Rev. 81:898

64. Nemirovsky, P. E., Adamchuk, Y. V. (1962). Nucl. Phys. 39:551

65. Huizenga, J. R., Vonach, H. K., Katsanos, A. A., Gorski, A. J., Stephan, C. J. 1969. Phys. Rev. 182:1149

66. Katsanos, A. A., Shaw, R. W., Jr., Vandenbosch, R., Chamberlin, D. 1970. Phys. Rev. C1:594

67. Vonach, A. K., Katsanos, A. A., Huizenga, J. R. 1968. Nucl. Phys. A122:465

68. Vonach, H. K., Hille, M. 1969. Nucl. Phys. A127:289

69. Maruyama, M. 1969. Nucl. Phys. A131:145

70. Ignatyuk, A. V., Stavinskii, V. S., Shubin, Yu. N. 1970. Sov. Journ. of Nucl. Phys. 11:563

71. Brookhaven National Laboratory Report BNL-325, II Edition Supplement No. 2, 1965-1966

72. Lynn, J. W. 1968. The Theory of Neutron Resonance Reactions,

Clarendon Press, Oxford

73. Facchini, U., Saetta-Menichella, E. 1968. Energia Nucleare 15:54

74. Baba, H., Baba, S. 1969. JAERI-1183

75. Erba, E., Facchini, U., Saetta-Menichella, E. 1961. Nuovo Cimento 22:1237

76. Lang, D. W. 1961. Nucl. Phys. 26:434. 1966 Nucl. Phys. 77:545

77. Browne, J. C., Newson, H. W., Bilpuch, E. G., Mitchell, G. E. 1970. Nucl. Phys. A153:481

78. Endt, P. M., van der Leun, C. 1967. Nucl. Phys. A105:1

79. Bilpuch, E. G. (1972). Statistical Properties of Nuclei, Edited by J. B. Garg, Plenum Press (New York) p. 99

80. Keyworth, G. A., Kyker, G. C. Jr., Bilpuch, E. G., Newson, H. W. (1966). Nucl. Phys. 89:590

81. Browne, J. C., Keyworth, G. A., Lindstrom, D. P., Moses, J. D., Newson, H. W., Bilpuch, E. G. 1968. Phys. Letters 28B:26

82. Wilhjelm, P., Keyworth, G. A., Browne, J. C., Beres, W. P. Divadeenam, M., Newson, H. W., Bilpuch, E. G. 1969. Phys. Rev. 177:1553

83. Prochnow, N. H., Newson, H. W., Bilpuch, E. G., Mitchell, G. E., to be published

84. Moses, J. D., Newson, H. W., Bilpuch, E. G., Mitchell, G. E., 1972. Nucl. Phys. to be published

85. Lindstrom, D. P., Newson, H. W., Bilpuch, E. G. 1971. Nucl. Phys. A168:37

86. Browne, J. C., Lindstrom, D. P., Moses, J. D., Newson, H. W., Bilpuch, E. G., Mitchell, G. E. 1969. Nuclear Isospin, Academic Press, Inc. (New York) p. 573

87. Lu, C. C., Vaz, L. C., Huizenga, J. R. 1972. Nucl. Phys. to be published

88. Vonach, H. K., private communication

89. Katsanos, A. A., Huizenga, J. R. 1967. Phys. Rev. 159:931

90. Lu, C. C., Vaz, L. C., Huizenga, J. R., to be published

91. Wigner, E. P. 1957. Gatlinburg Conference on Neutron

Physics by time-of-flight, ORNL-2309, p. 59

92. Rosenzweig, N., Porter, C. E. 1960. Phys. Rev. 120:1098

93. Huizenga, J. R., Katsanos, A. A. 1967. Nucl. Phys. A98:614

94. Allas, R. G., Meyer-Schützmeister, L., Von Ehrenstein, D. 1965. Nucl. Phys. 61:289

95. Grace, M. A., Poletti, A. R. 1966. Nucl. Phys. 78:273

96. Bjerregaard, J. H., Dahl, P. F., Hansen, O., Sidenius, S. 1964. Nucl. Phys. 51:641

97. Brown, G., MacGregor, A., Middleton, R. 1966. Nucl. Phys. 77:385

98. MacGregor, A., Brown, G., 1966. Nucl. Phys. 88:385

99. Mazari, M., Buechner, W. W., Sperduto, A. 1958. Phys. Rev. 112:1692

100. Aspinall, A., Brown, G., Warren, S. E. 1963. Nucl. Phys. 46:33

101. Katsanos, A. A., Huizenga, J. R., Vonach, H. K. 1966. Phys. Rev. 141:1053

102. Brown, G., Warren, S. E., Middleton, R. 1966. Nucl. Phys. 77:365

103. Sperduto, A., Buechner, W. W. 1964. Phys. Rev. 134:B142

104. Gadioli, E., Recami, E., Zetta, L. 1969. Nucl. Phys. A128 A128:339

105. Lederer, C. M., Hollander, J. M., Perlman, I. 1967. Table of Isotopes, John Wiley & Sons, Inc.

106. Nuclear Data Sheets, 1959-65. Nuclear Data, Section A, Vol. 1-8, 1965-1971, Section B, Vol. 1-5, 1966-1971

107. Gadioli, E., Zetta L. 1968. Phys. Rev. 167:1016

108. Douglas, A. C., MacDonald, N. 1959. Nucl. Phys. 13:382

109. Wolfstein, L. 1951. Phys. Rev. 82:690

110. Hauser, W., Feshbach, H. 1952. Phys. Rev. 87:366

111. Lane, A. M., Thomas, R. G. 1958. Rev. of Mod. Phys. 30:257

112. Ericson, T., Strutinsky, V. 1958. Nucl Phys. 8:284; 1958-1959. Nucl. Phys. 9:689

113. Thomas, T. D. 1968. Ann. Rev. of Nucl. Sci. 18:343

114. Thomson, D. B. 1963. Phys. Rev. 129:1649

115. Tsukada, K., Tanaka, S., Maruyama, M., Tomita, Y. 1966. Nucl. Phys. 78:369

116. Sal'nikov, O. A., et. al. 1971. Sov. Journ. Nucl. Phys. 12:620

117. Buccino, S. G., Hollandsworth, C. E., Lewis, H. W., Bevington, P. R. 1964. Nucl. Phys. 60:17

118. Owens, R. O., Towle, J. H. 1968. Nucl. Phys. A112:337

119. Hansen, L. F., Albert, R. D. 1962. Phys. Rev. 128:291

120. Alvra, A. et. al. 1964. Nucl. Phys. 58:108

121. Anufrienko, V. B. et. al. 1966. Sov. Journ. Nucl. Phys. 2:589

122. Bramblett, R. L., Bonner, T. W. 1960. Nucl. Phys. 20:395

123. Colli, L., Facchini, U., Micheletti S. 1957. Nuovo Cimento 5:502

124. Colli, L., Cuelbar, F., Micheletti, S., Pignanelli, M. 1959. Nuovo Cimento 14:81

125. Colli L., Facchini, U., Iori, I., Marcazzan, M. G., Sona, A. M. 1959. Nuovo Cimento 13:730

126. Dryapachenko, I. P., Kornilov, V. A., Nemetz, O. F., Pilipchenko, V. A. 1968. Sov. Journ. Nucl. Phys. 6:321

127. Graves, E. R., Rosen, L. 1953. Phys. Rev. 89:343

128. Kumake, I., Fink, R. W. 1960. Nucl. Phys. 15:316

129. Cindro, N. 1966. Rev. Mod. Phys. 38:391

130. Allan, D. L. 1961. Nucl. Phys. 24:274

131. Dixon, W. R. 1963. Nucl. Phys. 42:27

132. Facchini, U., Saetta-Menichella E., Tonolini, F., Tonolini-Severgnini, L. 1964. Nucl. Phys. 51:460

133. Holbrow, C. H., Barschall, H. H. 1963. Nucl. Phys. 42:264

134. Magda, M. T. et. al. 1970. Nucl. Phys. A140:23

135. Schectman, R. M., Anderson, J. D. 1966. Nucl. Phys. 77:241

136. Seth, K. K., Wileznick, R. M., Griffy, T. A. 1964. Phys. Letters 11:308

137. Sidorov, V. A. 1962. Nucl Phys. 35:253

138. Stavinskii, V. S. 1971. Sov. Journ. Nucl. Phys. 12:523

139. Stavinskii, V. S. 1970. Sov. Journ. Nucl. Phys. 11:338

140. Thomas, T. D. 1964. Nucl. Phys. 53:558; 1964 Nucl. Phys.

53:577

141. Wood, R. M., Borchers, R. R., Barschall, H. H. 1965. Nucl. Phys. 71:529

142. Wong, C., Anderson, J. D., McClure, J. W., Walker, B. D. 1964. Nucl. Phys. 57:515

143. Grimes, S. M., Anderson, J. D., McClure, J. W., Pohl, B. A., Wong, C. 1971. Phys. Rev. 3C:645

144. Grimes, S. M., Anderson, J. D., Pohl, B. A., McClure, J. W., Wong, C. 1971. Phys. Rev. 4C:607

145. Plattner, R., Huber, P., Poppelbaum, C., Wagner, R. 1963. Helv. Phys. Acta. 36:1059

146. Huber, P., Plattner, R., Poppelbaum, C., Wagner, R. 1963. Phys. Letters 5:202

147. Sobottka, H. et. al. Helv. Phys. Acta. 43:559

148. Mathur, S. C., Buchanan, P. S., Morgan, I. L. 1969. Phys. Rev. 186:1038

149. Lassen, N. O., Sidorov, V. A. 1960. Nucl. Phys. 19:579

150. Cohen, B. L., Rubin, A. G. 1959. Phys. Rev. 113:579

151. Bodansky, D. 1962. Ann. Rev. Nucl. Sci. 12:79

152. Fulbright, H. W., Lassen, N. O., Paulsen, N. O. R. 1959. Mat. Fys. Medd. Dan. Vid. Selsk. 31:No. 10

153. Gugelot, P. C. 1954. Phys. Rev. 93:425

154. Gadioli, E., Zetta, L. 1967. Nuovo Cimento 51:1074

155. Ignatyuk, A. V., Shorin, V. S. 1971. Sov. Journ. Nucl. Phys. 12:660

156. Patzak, W., Vonach, H. 1962. Nucl. Phys. 39:263

157. Lang, D. W. 1961, Nucl. Phys. 26:434

158. Hurwitz, C., Spencer, S. J., Esterlund, R. A., Pate, B. D., Reynolds, J. B. 1964. Nucl. Phys. 54:65

159. Kulisic, P., Ajdacic, V., Cindro, N., Lalovic, B., Strohal, P. 1964. Nucl. Phys. 54:17

160. Kennedy, A. J., Pacer, J. C., Sprinzak, A., Wiley, J., Porile, N. T. 1972. Phys. Rev. 5C:500

161. Sherr, R., Brady, F. P. 1961. Phys. Rev. 124:1928

162. Seebeck, U., Bormann, M. 1965. Nucl. Phys. 68:387

163. Saetta-Menichella, E., Tonolini, F., Tonolini-Severgnini

L. 1964. Nucl. Phys. 51:449

164. Turkiewicz, I. M., Cindro, N., Kulisic, P., Strohal, P., Veselic, D. 1966. Nucl. Phys. 77:276

165. Vonach, H. K., Huizenga, J. R. 1966. Phys. Rev. 149:844

166. Williams, D. C., Thomas, T. D. 1967. Nucl. Phys. A92:1; 1968. Nucl. Phys. A107:552

167. Swenson, L. W., Gruhn, C. R. 1966. Phys. Rev. 146:886

168. Swenson, L. W., Cindro, N. 1961. Phys. Rev. 123:910

169. Ahrens, S. T., Simon, W. G., Eldridge, H. B. 1970. Phys. Rev. 2C:1433

170. Benveniste, J., Merkel, G., Mitchell, A. 1966. Phys. Rev. 141:980; 1968. Phys. Rev. 174:1357; 1970. Phys. Rev. 2C:500

171. Chenevert, G., Halpern, I., Harvey, B. G., Hendrie, D. L. 1968. Nucl. Phys. A122:481

172. Griffin, J. J. 1966. Phys. Rev. Letters 17:478

173. Blann, M. 1968. Phys. Rev. Letters 21:1357

174. Harp, G. D., Miller, J. M., Berne, B. J. 1968. Phys. Rev.

165:1166

175. Cline, C. K., Blann, M. 1971. Nucl. Phys. A172:225

176. Vonach, H. K., Huizenga, J. R. 1965. Phys. Rev. 138:B1372

177. Richter, A., von Witsh, W., von Brentano, P., Hausser, O., Mayer-Kuckuk, T., 1965. Phys. Letts. 14:121

178. Ericson, T., Mayer-Kuckuk, T. 1966. Ann. Rev. Nucl. Sci. 16:183

179. Braga-Marcazzan, G. M., Milazzo-Colli, L. 1968. Energia Nucleare 15:186; 1970. Prog. in Nucl. Phys. 11:145

180. Eberhard, K. A., Richter, A. 1972. Statistical Properties of Nuclei, Edited by J. B. Garg, Plenum Press (New York) p. 139

181. Maruyama, M. et. al. 1970. Nucl. Phys. A145:581

182. Temmer, G. M., Maruyama, M., Mingay, D. W., Petrascu, M., Van Bree, R. 1971. Phys. Rev. Letts. 26:1341

183. Clark, G. J. et. al. 1971. Nucl. Phys. A173:73

184. Gibson, W. M., Hashimoto, Y., Keddy, R. J., Maruyama, M., Temmer, G. M. To be published

185. Huizenga, J. R., Vandenbosch, R. 1960. Phys. Rev. 120:1305

186. Vandenbosch, R., Huizenga, J. R. 1960 Phys. Rev. 120:1313

187. Coceva, C., Corvi, F., Giacobbe, P., Stefanon, M. 1972. Statistical Properties of Nuclei, Edited by J. B. Garg, Plenum Press (New York) p. 447

188. Bormann, M., Bissem, H. H., Magiera, E., Warnemünde, R. 1970. Nucl. Phys. A157:481

189. We thank Dr. J. R. Nix for calculating these levels for us. Bolsterli, M., Fiset, E. O., Nix, J. R., Norton, J. L. 1972. Phys. Rev. C5:1050

FIGURE CAPTIONS

Fig. 1. Theoretical level densities as a function of excitation energy for nuclei in the neighborhood of the ^{208}Pb doubly closed shell (Ref. 40). The Nilsson shell model has been used to obtain the spherical set of single particle levels.

Fig. 2. Theoretical spin cut-off parameters σ^2 as a function of excitation energy for nuclei in the ^{208}Pb region (Ref. 40). The calculations have been performed on the basis of the Nilsson diagram.

Fig. 3. Energy intercepts ΔE of the tangents to the function S^2 vs E (left scale) for the nucleus ^{124}Pd; proton chemical potential (right scale) as a function of excitation energy (Ref. 57).

Fig. 4. Contour map of the gap parameter Δ as a function both of temperature T and angular momentum M. The spacing in Δ between two successive lines is 0.05 MeV from Δ = 1.0 MeV at the origin to Δ = 0.1 MeV. The outer line corresponds to Δ = 0. The calculation has been performed on the basis

of the equidistant model. The density of the doubly degenerate single particle states is 7 MeV^{-1} and the spin projection of the single particle levels is 2ℏ (Ref. 47).

Fig. 5. a) Potential energy as a function of deformation for the nucleus ^{172}Yb. The solid line represents the prediction of the liquid drop model, while the dotted line is calculated from the Nilsson model and the Strutinski procedure. b) Natural logarithms of the deformation probabilities for ^{172}Yb at excitation energies ranging from 6 MeV to 60 MeV (Ref. 49).

Fig. 6. Level density parameter $\underline{a}$ as a function of atomic mass A (Ref. 52).

Fig. 7. Spectrum of protons inelastically scattered from ^{56}Fe. The numbered lines represent excited levels in ^{56}Fe (Ref. 101).

Fig. 8. Experimental spacing distribution for 622 levels with $\overline{S} \geq 30$ keV. The data for $(S/\overline{S}) \geq 0.25$ are normalized to and compared with an exponential spacing distribution (Ref. 93).

Fig. 9. Dependence of the level density parameter $\underline{a}$ deduced

from the conventional approximate theory on the parameter n [see Equation (45)]. The theoretical spectra analyzed in this figure are calculated with Equations (37-39) and a level density of the form given by Equation (14). The input values of $\underline{a}$ used in the computation of the theoretical spectra are 6.8 and 5.8 MeV^{-1} for the residual nuclei ^{63}Cu and ^{60}Ni, respectively (Ref. 87).

Fig. 10. Analyses of theoretical neutron spectra from the $^{103}Rh(p,n)^{103}Pd$ reaction with the approximate constant temperature theory. The theoretical spectra are calculated with Equations (37-39) and analyzed with Equation (46). The theoretical and experimental temperatures are shown as a function of bombarding energy (Ref. 52).

Fig. 11. Plot of the experimental level density of ^{60}Ni as a function of excitation energy (Ref. 87).

Fig. 12. Comparison of theoretical and experimental values of σ. The solid lines are based on Nilsson single particle levels. The dashed line for ^{56}Fe is calculated for a set of single particle levels based on a potential very similar to that of

a Woods-Saxon potential (189). The dot-dashed lines are based on the rigid-body moments of inertia (Ref. 90).

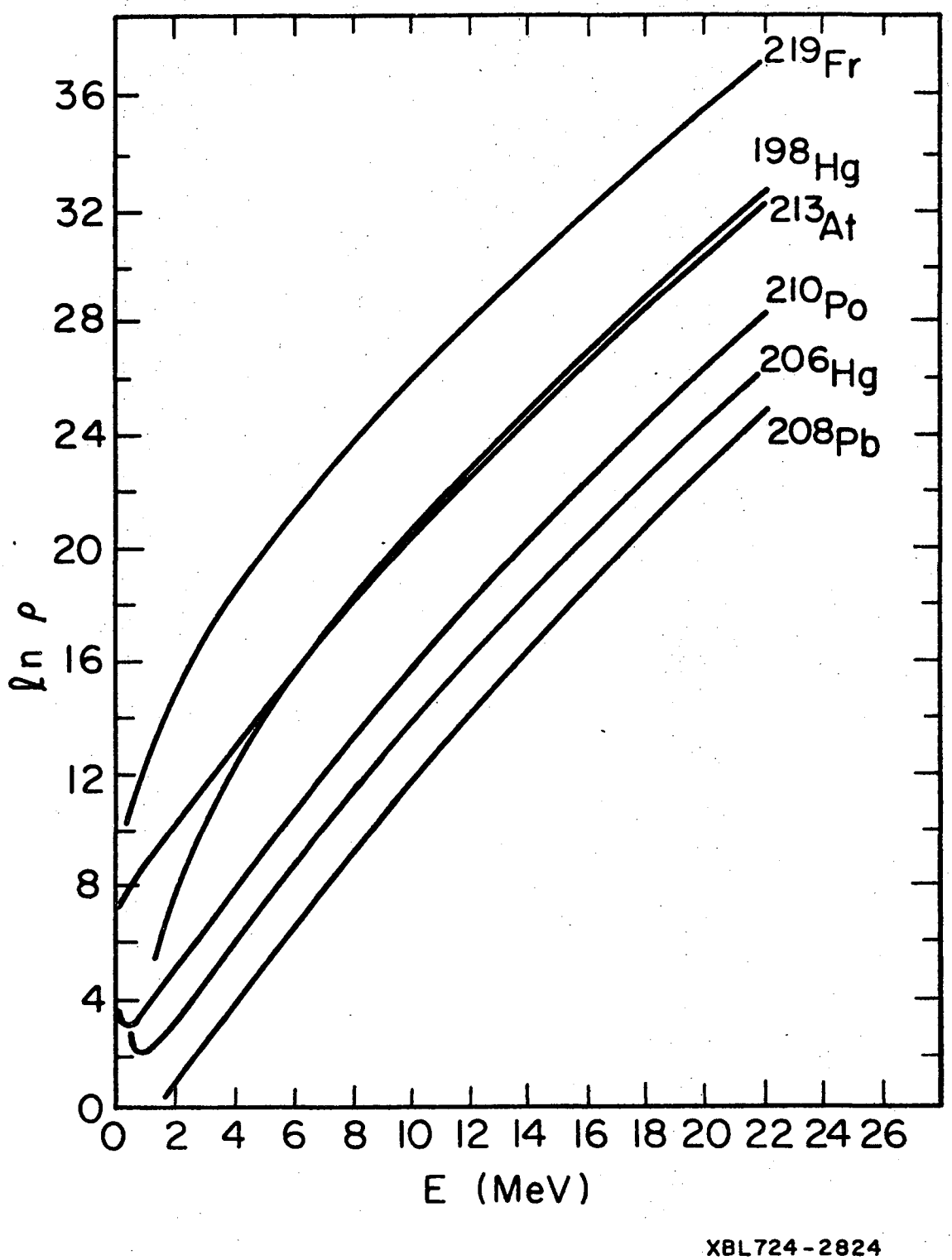
219Fr
198Hg
213At
210Po
206Hg
208Pb
ln ρ
0
4
8
12
16
20
24
28
32
36
0 2 4 6 8 10 12 14 16 18 20 22 24 26
E (MeV)
XBL724-2824

Fig. 1

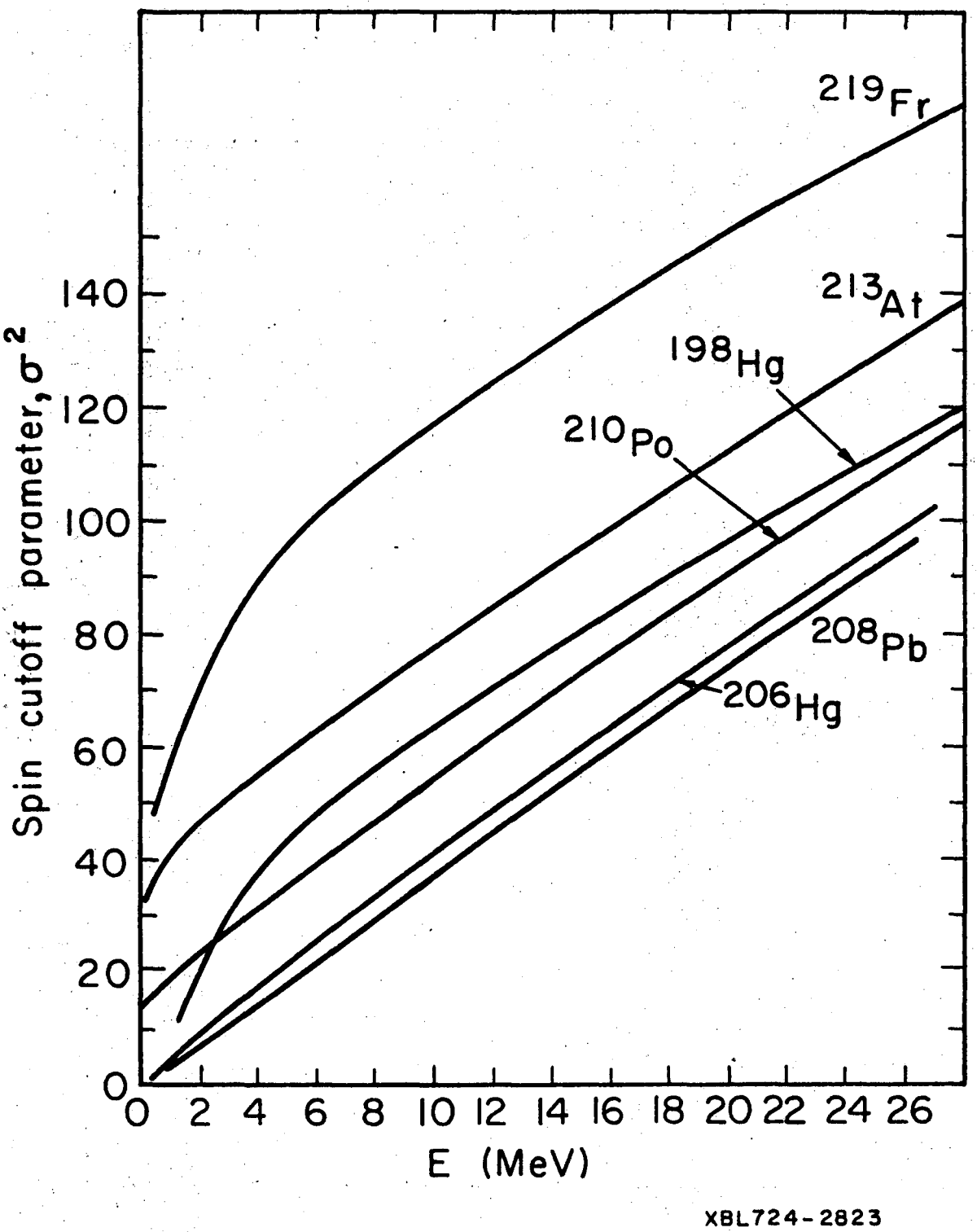
219Fr
213At
198Hg
210Po
208Pb
206Hg
Spin cutoff parameter, σ²
0
20
40
60
80
100
120
140
0 2 4 6 8 10 12 14 16 18 20 22 24 26
E (MeV)
XBL724-2823

Fig. 2

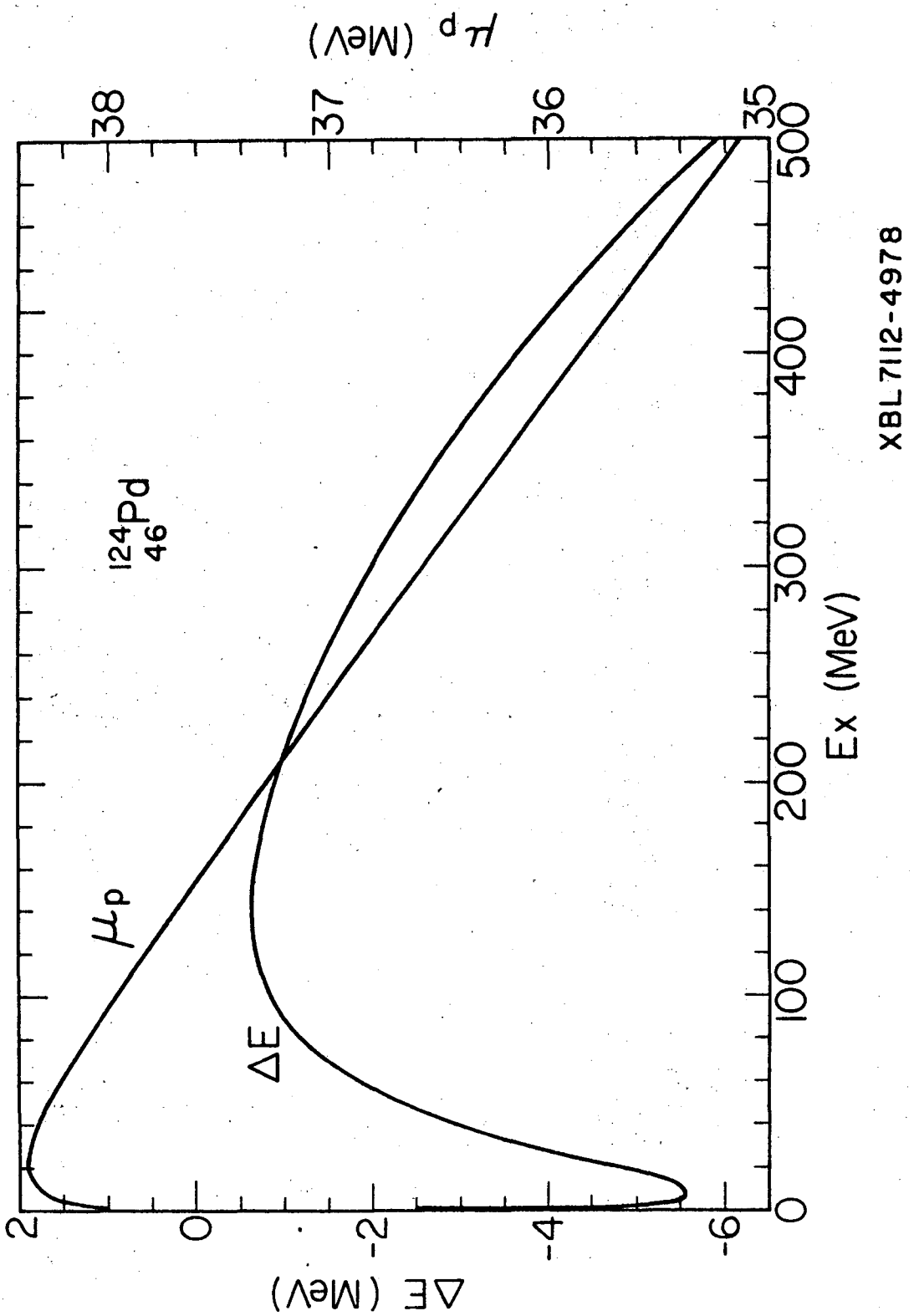
μ_p (MeV)
38
37
36
35
500
400
300
200
100
0
Ex (MeV)
$^{124}_{46}Pd$
μ_p
ΔE
2
0
-2
-4
-6
ΔE (MeV)
XBL7112-4978

Fig. 3

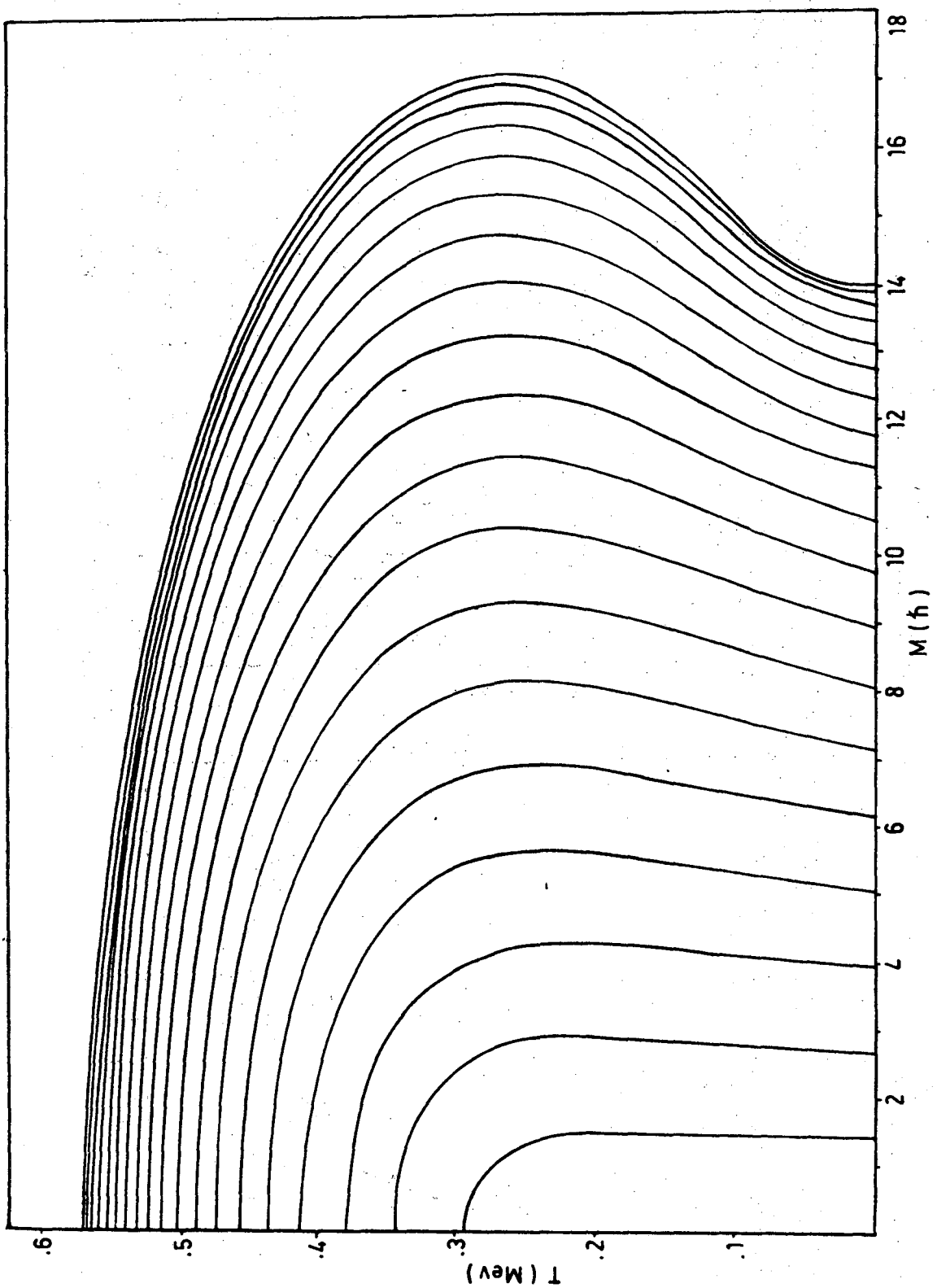

Fig. 4

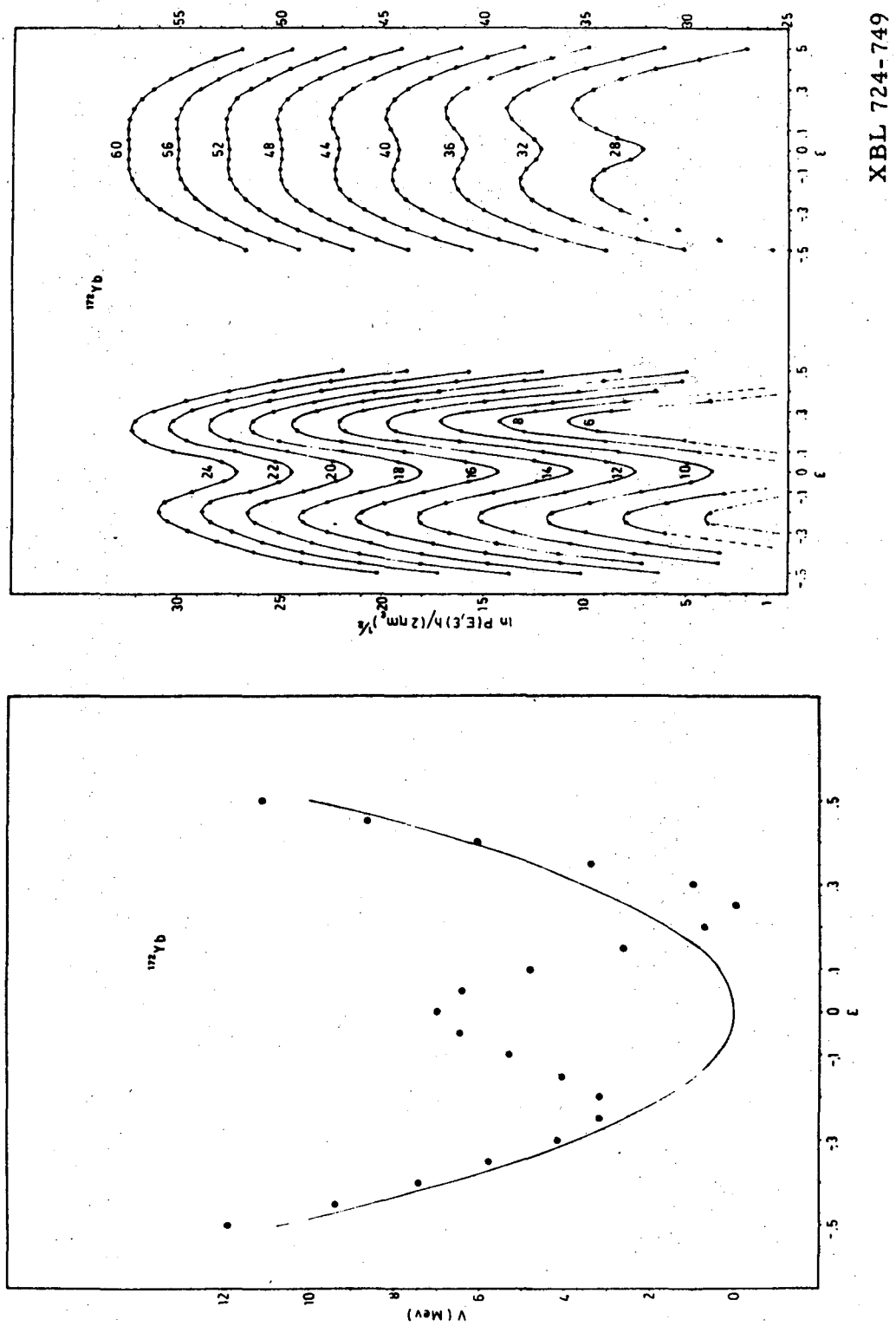

Fig. 5

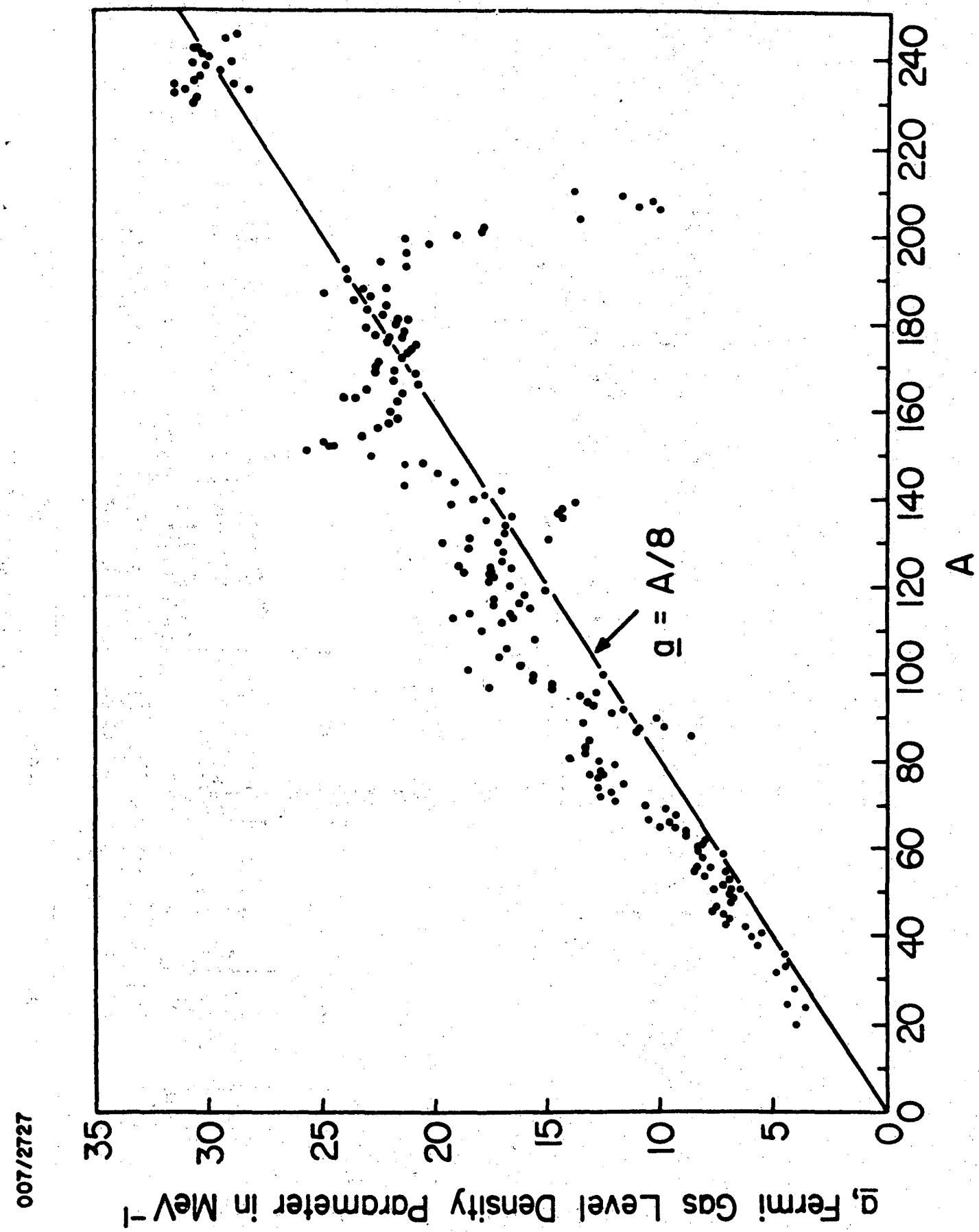

Fig. 6

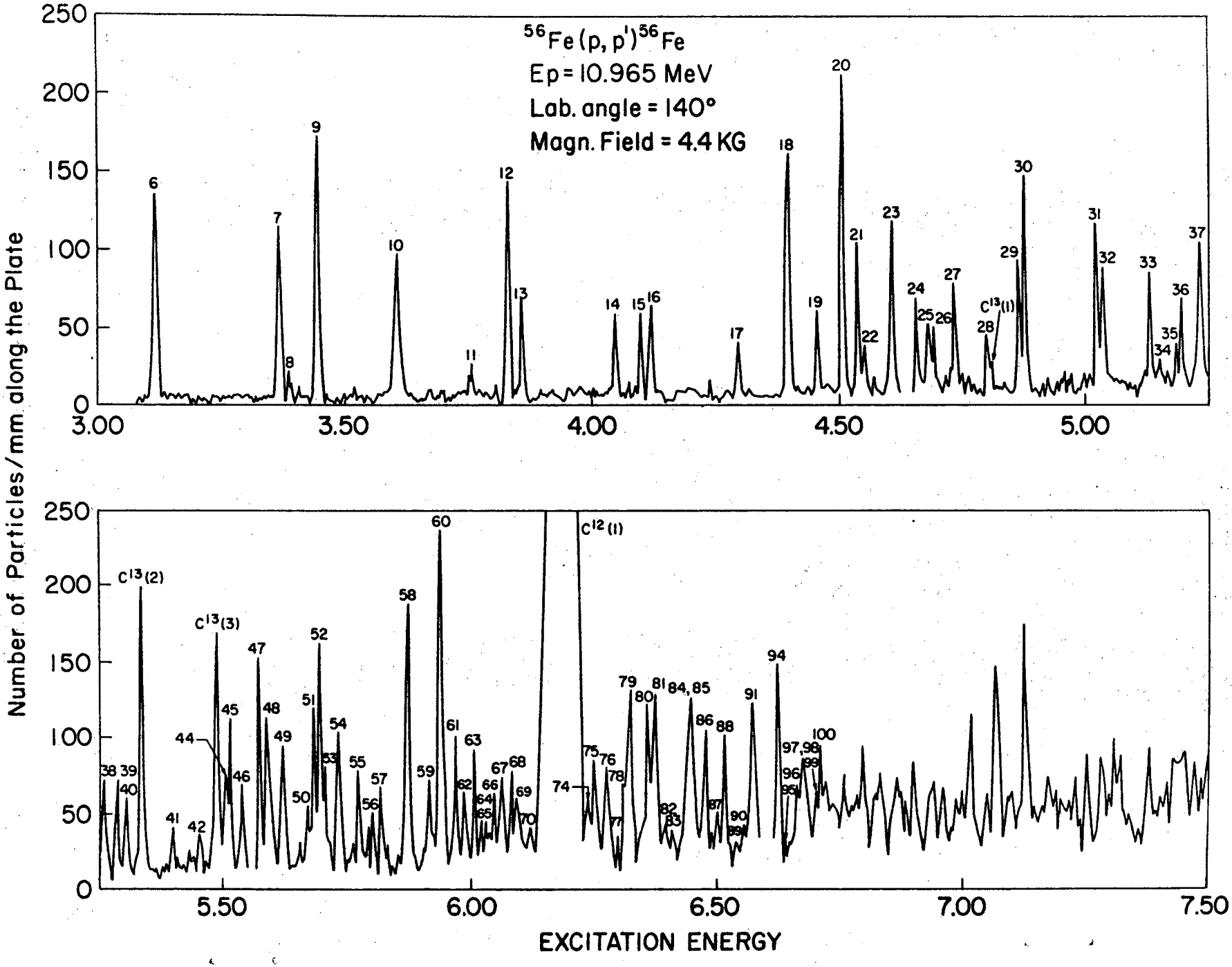
$^{56}Fe(p, p')^{56}Fe$
Ep = 10.965 MeV
Lab. angle = 140°
Magn. Field = 4.4 KG
Number of Particles/mm along the Plate
EXCITATION ENERGY
C13(1)
C13(2)
C13(3)
C12(1)

Fig. 7

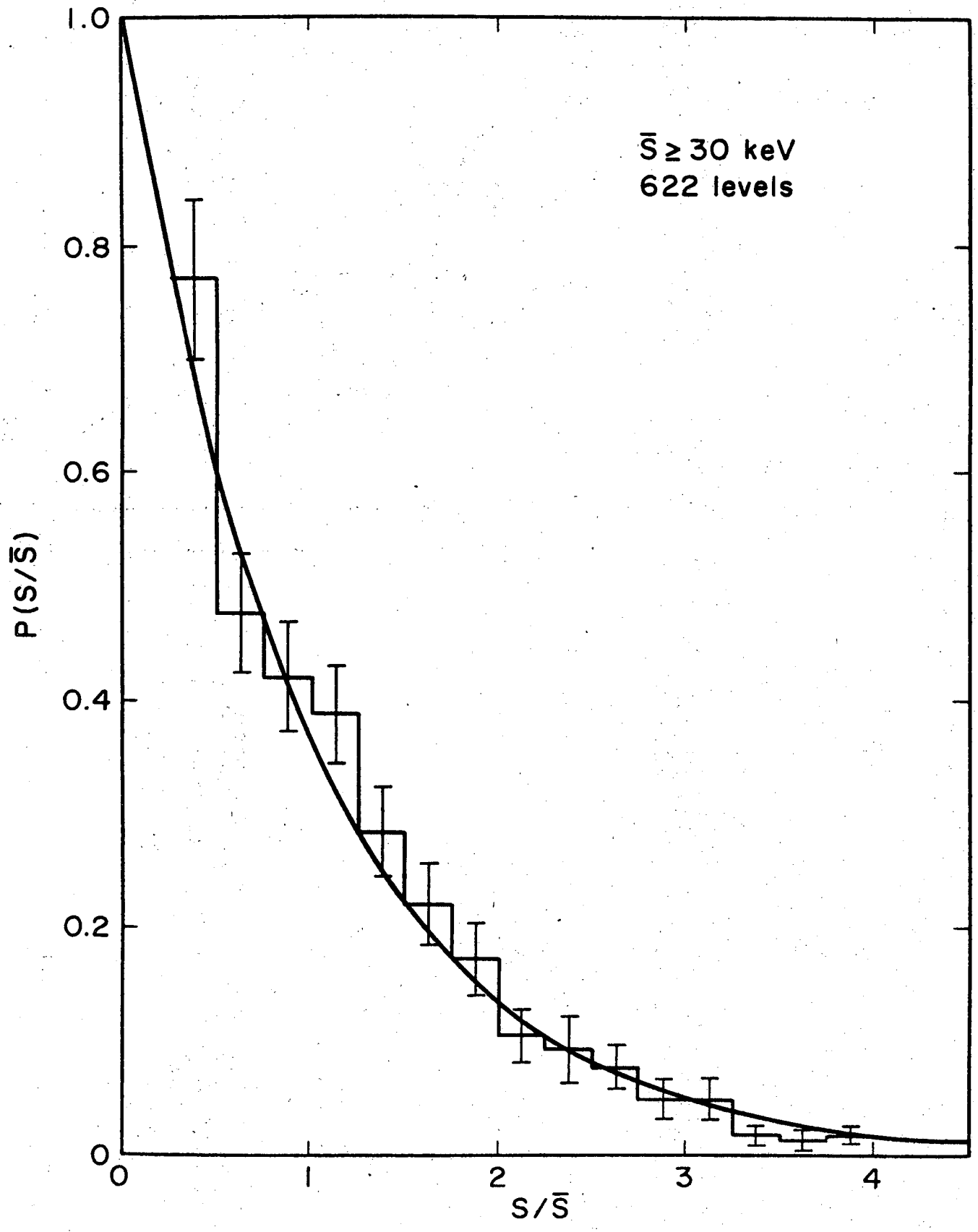

Fig. 8

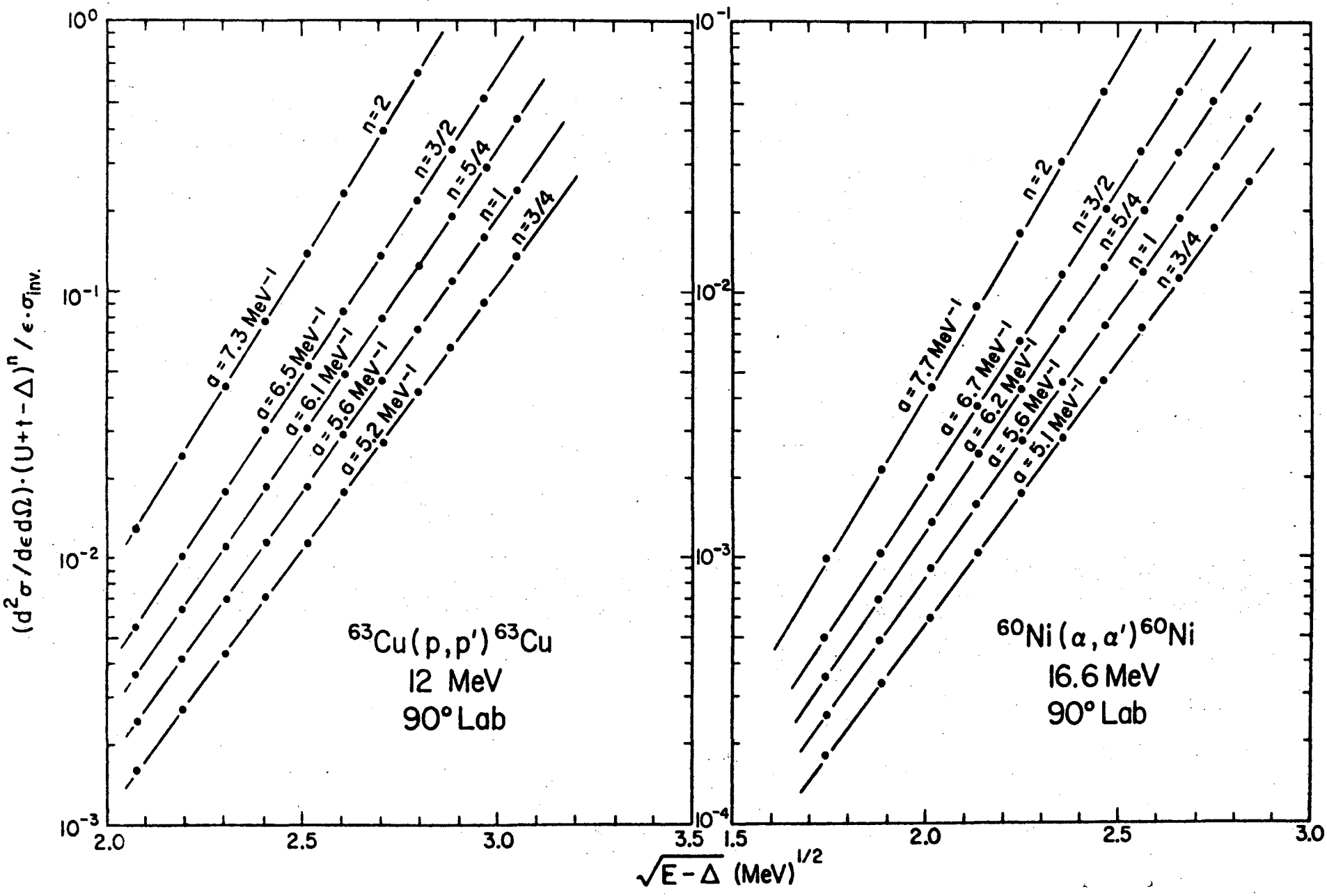
$(d^2\sigma/d\epsilon d\Omega)\cdot(U+t-\Delta)^n/\epsilon\cdot\sigma_{inv.}$
$\sqrt{E-\Delta}$ (MeV)$^{1/2}$
^{63}Cu(p,p')^{63}Cu
12 MeV
90° Lab
a=7.3 MeV^{-1}
a=6.5 MeV^{-1}
a=6.1 MeV^{-1}
a=5.6 MeV^{-1}
a=5.2 MeV^{-1}
n=2
n=3/2
n=5/4
n=1
n=3/4
^{60}Ni(α,α')^{60}Ni
16.6 MeV
90° Lab
a=7.7 MeV^{-1}
a=6.7 MeV^{-1}
a=6.2 MeV^{-1}
a=5.6 MeV^{-1}
a=5.1 MeV^{-1}
n=2
n=3/2
n=5/4
n=1
n=3/4

Fig. 9

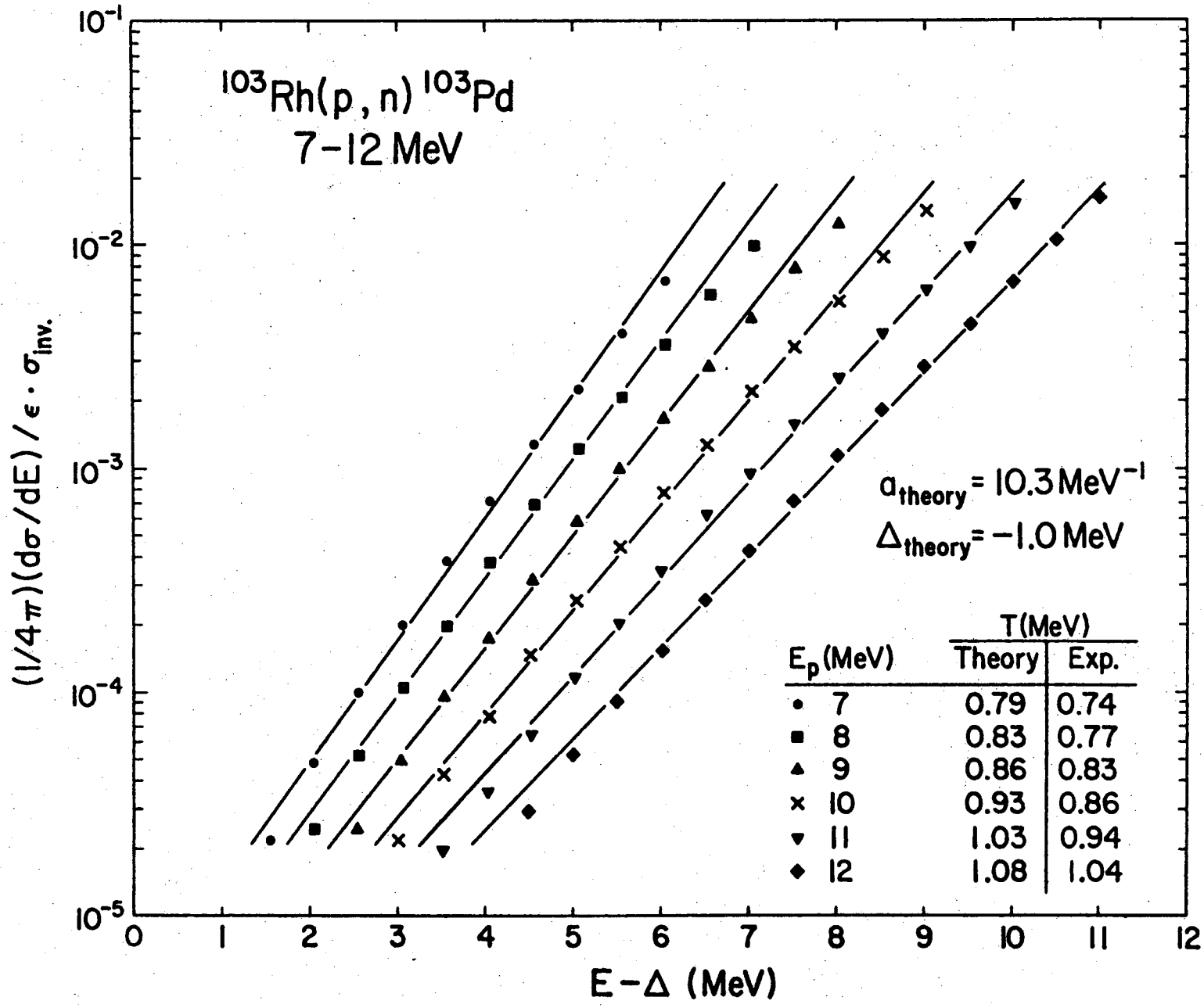
^{103}Rh(p, n) ^{103}Pd
7–12 MeV
a_{theory} = 10.3 MeV^{-1}
Δ_{theory} = −1.0 MeV
T(MeV)
E_p(MeV) Theory Exp.
7 0.79 0.74
8 0.83 0.77
9 0.86 0.83
10 0.93 0.86
11 1.03 0.94
12 1.08 1.04
$(1/4\pi)(d\sigma/dE)/\epsilon \cdot \sigma_{inv.}$
E−Δ (MeV)

Fig. 10

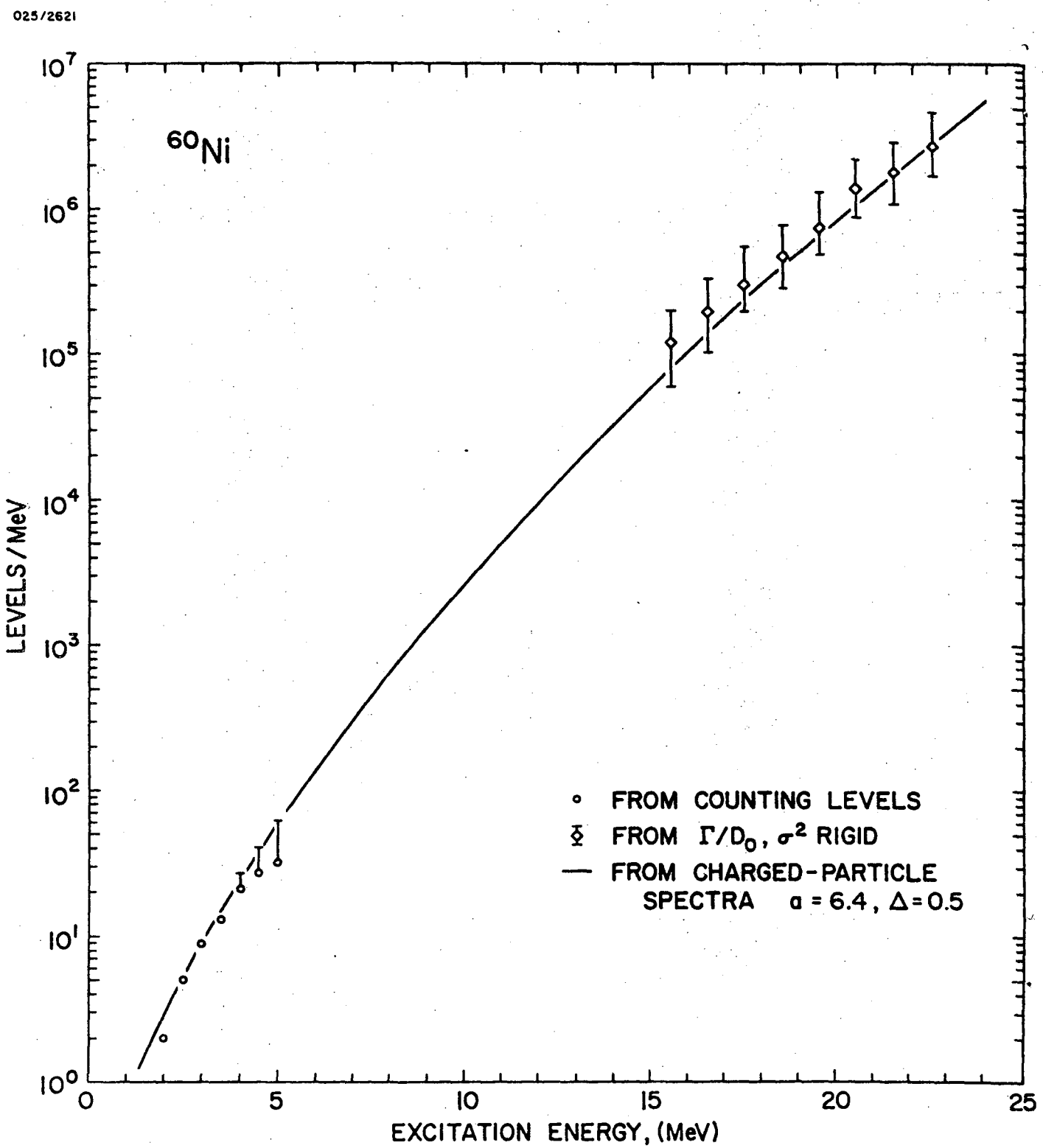
025/2621
^{60}Ni
LEVELS/MeV
EXCITATION ENERGY, (MeV)
FROM COUNTING LEVELS
FROM Γ/D_0, σ^2 RIGID
FROM CHARGED-PARTICLE SPECTRA a = 6.4, Δ = 0.5

Fig. 11

007/3002

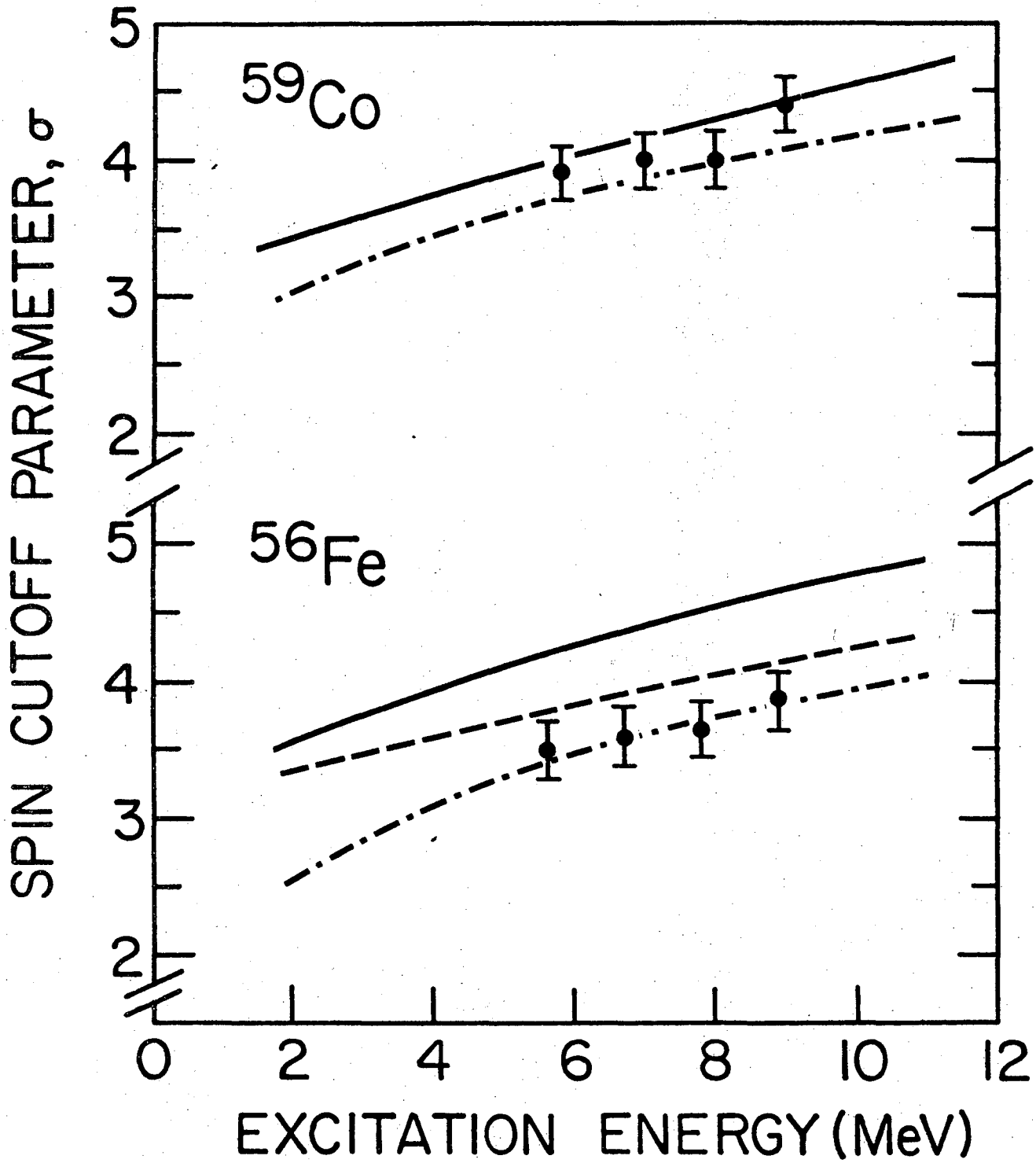

Fig. 12

TECHNICAL INFORMATION DIVISION
LAWRENCE BERKELEY LABORATORY
UNIVERSITY OF CALIFORNIA
BERKELEY, CALIFORNIA 94720